OTH Amberg-Weiden

DLR Deutsches Zentrum für Luft- und Raumfahrt
German Aerospace Center

Master Thesis

Energy Saving Potential of IR Heating with Reflective Walls Compared to Conventional Systems: A Building Energy Simulation Study

by

Vasimraza Kaji

International Energy Engineering
Faculty of Mechanical and Environmental Engineering
Ostbayerische Technische Hochschule Amberg-Weiden

University Examiner:	Prof. Dr. Raphael Lechner
External Examiner:	Lukas Wille

Date of Issue:	August 01, 2025
Submission Date:	January 15, 2026

Ostbayerische Technische Hochschule Amberg-Weiden
Faculty of Mechanical and Environmental Engineering

Confirmation in accordance with §27 ASPO Sec. (9)

Name and first name of the student: **Kaji, Vasimraza**

Degree program: **International Energy Engineering**

I hereby confirm that I have written the Master Thesis entitled:

Energy Saving Potential of IR Heating with Reflective Walls Compared to Conventional Systems: A Building Energy Simulation Study

independently, have not submitted it elsewhere for examination purposes, have used no sources or aids other than those indicated, and have marked literal and analogous quotations as such. AI tools were used to support the creation of this text.

Date: January 15, 2026

Signature:

Ostbayerische Technische Hochschule Amberg-Weiden
Faculty of Mechanical and Environmental Engineering

Master Thesis Summary

Student (Last name, First name):	**Kaji, Vasimraza**
Degree program:	International Energy Engineering
Supervisor, Professor:	Prof. Dr. Raphael Lechner
Conducted at (Company/Institution/University):	DLR Institute of Solar Research
Industry supervisor:	Lukas Wille
Start date: August 01, 2025	Submission date: January 15, 2026

Title:

Energy Saving Potential of IR Heating with Reflective Walls Compared to Conventional Systems: A Building Energy Simulation Study

Summary

This thesis evaluates an infrared heating strategy combined with reflective wall surfaces as an alternative to conventional heating systems. EnergyPlus simulations are performed for a high-demand single zone house and a low-demand hotel guestroom. The new heating approach is assessed across different envelope qualities, climate types, and occupancy patterns. The infrared heater is controlled via an Energy Management System based on a PMV regression function. The results show that the proposed strategy can significantly reduce heating energy use, greenhouse gas emissions, and operational fuel costs. Particularly, the combination of cold climate, poor insulation, and short duration occupancy produced the largest absolute savings. The highest energy savings of 37% for the house model and 56% for the hotel guestroom are noticed. Across all scenarios, maximum absolute reductions of about 31% in GHG emissions and 24% in operational fuel costs are observed. However, longer operating hours of the IR heater increase fuel costs and reduce these benefits. Overall, the findings demonstrate the strong potential of this new infrared heating as an efficient and low-emission solution for building heating applications.

Keywords

IR heating, reflective surfaces, energy saving, EMS, EnergyPlus

Acknowledgment

I would like to take this opportunity to thank everyone who contributed to the completion of this thesis.

I would like to express my sincere gratitude to my university supervisor, Prof. Raphael Lechner, for his valuable guidance, feedback, and continuous support throughout this work.

I am especially grateful to my supervisor at DLR, Lukas Wille, for his dedicated supervision, constant support, and willingness to discuss ideas, questions, and challenges at every stage of the research. His experimental work and guidance created a strong foundation for this study.

I would also like to thank the buildings and districts research group at DLR for providing a supportive and motivating working environment. The valuable discussions, feedback, and thoughtful questions during progress meetings greatly improved this work.

Finally, I would like to express my heartfelt gratitude to my family for their unconditional love, support, and encouragement throughout my studies. Their trust in me has been a constant source of motivation. Without them, this accomplishment would not have been possible.

Abstract

Reducing heating energy demand is the primary requirement for achieving a decarbonized building stock. By utilizing reflective surfaces, radiant heat can be directed more effectively toward occupants, enabling lower air temperature setpoints and therefore reducing energy use. This study investigates the energy saving potential of an infrared (IR) heating strategy combined with reflective walls compared to conventional heating systems.

The comparison is evaluated with respect to energy end use, greenhouse gas emissions, and operational fuel costs. Two building models are analyzed using EnergyPlus: a high-demand single zone house and a low-demand hotel guestroom. The comparison is performed across different envelope qualities (old vs. new construction), climate conditions (continental vs. maritime), and occupancy patterns (long vs. short duration). The IR heater is controlled through an Energy Management System (EMS) inside EnergyPlus, which regulates its power based on a PMV regression function and activates it immediately upon occupancy to provide quick thermal comfort.

The proposed IR strategy delivers substantial absolute reductions in energy end use. Maximum energy savings of 37% are observed for the house model, while the hotel guestroom achieves reductions of up to 56% compared to conventional gas heating. Cold climates and poorly insulated buildings, which represent high heating demand cases, show larger absolute savings and thus a greater climate impact. In contrast, the IR strategy gives small savings but runs more effectively in well-insulated buildings with lower heating demand. Across both models, maximum absolute reductions of about 31% in GHG emissions and 24% in operational fuel costs are observed. All maximum reductions occur with the short-duration occupancy, which consistently leads to energy, emission, and cost savings, whereas a longer occupancy pattern results in higher operational costs. Overall, the results demonstrate strong potential for this infrared heating concept as an efficient and low-emission alternative to conventional systems.

Zusammenfassung

Die Reduzierung des Heizenergiebedarfs ist eine zentrale Voraussetzung für die Dekarbonisierung des Gebäudebestands. Durch den Einsatz reflektierender Oberflächen kann Strahlungswärme gezielter auf die Nutzer gelenkt werden, wodurch niedrigere Lufttemperatur-Sollwerte möglich sind und der Energieverbrauch sinkt. Diese Arbeit untersucht das Energieeinsparpotenzial einer Infrarot-(IR)-Heizstrategie in Kombination mit reflektierenden Innenwänden im Vergleich zu konventionellen Heizsystemen.

Der Vergleich erfolgt hinsichtlich des Endenergieverbrauchs, der Treibhausgasemissionen und der betrieblichen Energiekosten. Zwei Gebäudemodelle werden mit EnergyPlus analysiert: ein Einzonen-Wohnhaus mit hohem Heizbedarf sowie ein Hotel-Gästezimmer mit niedrigem Heizbedarf. Die Untersuchung umfasst unterschiedliche Gebäudehüllen (Altbau und Neubau), Klimabedingungen (kontinental und maritim) sowie Belegungsmuster (lange und kurze Aufenthaltsdauer). Der IR-Heizer wird über ein Energy Management System (EMS) innerhalb von EnergyPlus geregelt, welches die Heizleistung auf Basis einer PMV-Regressionsfunktion steuert und den Heizbetrieb unmittelbar bei Belegung aktiviert, um schnell thermischen Komfort bereitzustellen.

Die vorgeschlagene IR-Strategie erzielt deutliche absolute Reduktionen des Endenergieverbrauchs. Für das Wohnhaus werden maximale Energieeinsparungen von 37% erreicht, während im Hotel-Gästezimmer Einsparungen von bis zu 56% gegenüber einer konventionellen Gasheizung beobachtet werden. Kalte Klimazonen und schlecht gedämmte Gebäude, die einen hohen Heizbedarf aufweisen, zeigen größere absolute Einsparungen und damit eine höhere Klimawirkung. Im Gegensatz dazu erzielt die IR-Strategie in gut gedämmten Gebäuden mit geringem Heizbedarf zwar absolut geringere Einsparungen, arbeitet dort jedoch besonders effizient. Über beide Gebäudemodelle hinweg werden maximale absolute Reduktionen von etwa 31% bei den Treibhausgasemissionen sowie bis zu 24% bei den betrieblichen Energiekosten festgestellt. Alle maximalen Einsparungen treten bei kurzer Aufenthaltsdauer auf, die durchweg zu Energie-, Emissions- und Kosteneinsparungen führt, während längere Belegungsmuster höhere Betriebskosten verursachen. Insgesamt zeigen die Ergebnisse ein hohes Potenzial dieses Infrarot-Heizkonzepts als effiziente und emissionsarme Alternative zu konventionellen Heizsystemen.

Contents

List of Figures

List of Tables

List of Abbreviations

ACH	Air Changes per Hour
ASHRAE	American Society of Heating, Refrigerating and Air-Conditioning Engineers
DOE	Department of Energy
EPW	EnergyPlus Weather
EMS	Energy Management System
Erl	EnergyPlus runtime language
EU	European Union
GHG	Greenhouse gas
HVAC	Heating, Ventilation and Air Conditioning
IDF	Input Data File
IR	Infrared
MRT	Mean Radiant Temperature
PMV	Predicted Mean Vote
PPD	Predicted Percentage Dissatisfied

1. Introduction

This chapter presents an overview of the thesis. It begins with the motivation behind the study, followed by a review of relevant literature, and concludes with a description of the research objective and a brief overview of the methodological approach.

1.1 Motivation

Buildings account for 30% of the world's total final energy consumption and 26% of global energy-related emissions [1]. In Europe, the building sector is the primary consumer of energy and contributes approximately 36% of total greenhouse (GHG) emissions, with a significant proportion required to maintain a comfortable indoor climate, particularly during winter [2]. The need to improve building performance becomes apparent considering that 85% of the buildings in the European Union (EU) were built before 2000. Furthermore, it is estimated that approximately 75% of the total buildings exhibit poor energy performance [3]. Enhancing the energy efficiency of these existing buildings is therefore crucial for conserving energy, lowering energy costs, and ultimately achieving a decarbonized building stock.

The European Climate Law sets the goal of achieving carbon neutrality, or net zero greenhouse gas emissions, by the end of 2050 [4]. The core objective behind this is to align with the Paris Agreement, which calls for limiting the increase in global average temperature to below 2 °C above pre-industrial levels. Most of the buildings must be highly energy efficient and have an Energy Performance Certificate grade of A in order to achieve a decarbonized building stock. According to the Buildings Performance Institute Europe research, fewer than 3% of buildings have been identified as having grade A [2]. Therefore, to meet the decarbonization target, almost 97% of buildings need to be renovated considering energy savings. However, in Germany, for instance, as per the report of the German Association of Energy-Efficient Building Envelopes, the current renovation rate remains below 1% per year and the trend indicates a further decline, highlighting the need for additional measures to modernize and decarbonize the current building stock [5].

While energy performance requirements successfully direct the construction of new buildings, enhancing the existing building stock remains significantly more demanding. The revised EU directives (2024) aim to accelerate renovation efforts, setting a target to reduce the average primary energy consumption of residential buildings by 16% by 2030 relative to 2020 levels [6].

To effectively reduce energy use in buildings, it is also essential to understand where energy is actually consumed within the building itself. According to EU statistics on final energy consumption in households [7], space heating alone is responsible for more than 60% of total end energy use as shown in Table 1.1. This shows that improving the efficiency of heating systems has a direct and substantial impact on reducing GHG emissions.

According to the recent assessment by the International Energy Agency (2025), Germany continues to rely heavily on natural gas and oil for space heating applications [8]. This reliance has become more concerning, especially following the disruption of fossil-fuel supply caused by the Russo–Ukrainian war [9]. These developments highlight the urgency of reducing fossil-fuel dependency. This way, since Germany continues to expand its renewable power gener-

Consumption type	Share
Space heating	62.5%
Water heating	15.1%
Lighting and appliances	14.5%
Cooking	6.5%
Other uses	1.4%

Table 1.1: Shown is the share of final energy consumption in households. [7]

ation capacity, the shift towards electricity driven heating technologies is becoming increasingly attractive. The country aims to achieve an 80% share of renewables in electricity generation by 2030 [8], which strengthens the case for electricity based heating solutions. Heat pumps, in particular, emerge as a highly efficient alternative to conventional fossil-fuel based systems, offering the potential for substantial reductions in greenhouse gas emissions [10].

However, the widespread deployment of heat pumps still faces several practical challenges. These include market barriers like a shortage of trained installers, and financial constraints that make integration into the existing building stock more difficult [11]. As the heating sector evolves, research efforts are increasingly focused on addressing these barriers, exploring innovative approaches such as hybrid heating systems and advanced control strategies that can further enhance energy efficiency [12]. In this context, electricity based heating technologies supported by smart energy management systems might play a crucial role in shaping the future of sustainable building heating.

1.2 Literature review

Radiant heating systems emit infrared (IR) radiation to directly transfer heat to objects and surfaces instead of heating air, as it occurs in convection-based systems [13, 14]. This direct heat transfer mechanism results in improved energy efficiency, with studies showing energy savings of 13–57% compared to conventional convective heaters. This way, it can provide comparable thermal comfort at lower air temperatures [15, 16, 17]. An experimental study inside an office room by Ali and Morsy (2010) [18] supports these findings. They found that radiant panel heaters can provide the same level of thermal comfort as conventional convective heaters with lower air temperatures, resulting in significant energy savings of up to 39.1%. The authors also noted that the placement of radiant panels has a significant impact on the thermal distribution within a radiantly heated room.

Simulation studies contribute to the experimental literature by highlighting where IR panels operate well and where they do not. Corsten (2021) [19] compared IR panels with heat pumps and gas boilers with floor heating for Dutch dwellings through a simulation based study. The results showed that all systems sustained indoor operational temperatures within the acceptable comfort range, yet the heat pump delivered the most stable conditions. Infrared panels produced greater radiant temperature asymmetry, especially in poorly insulated dwellings. On the other hand, they functioned significantly better in well-insulated homes. The study

concluded that IR panels are best suitable for well-insulated residences.

Field trials confirm these laboratory and simulation results in real buildings. TU Kaiserslautern carried out a five-month comparative study in an uninsulated two-family house [20]. The results showed that the gas heating system required roughly 2.5 times more energy than the IR heating to heat the same rooms. Similar IR heating supporting findings were reported in a recent field experiment by the Fraunhofer Institute for Building Physics, where wall-mounted electric infrared heaters were compared with a condensing gas boiler and flat radiators inside two identical twin houses over a 68-day winter period [15]. According to their results, the average indoor air temperature in the gas-heated dwelling was 0.4 K higher than in the IR-heated house. Over the same period, the IR-heated house consumed about 32% less energy compared to the gas heated reference house. However, the IR heating showed around 9% higher greenhouse gas emissions because of its electricity use.

Heider et al. also performed laboratory and field investigations, comparing infrared heating systems with underfloor heating driven by a heat pump in a multifamily building [17]. The results revealed that, at the same operative temperature, the air temperature in the IR heated room was 0.6 K lower than in the underfloor heated room, which results in fewer transmission heat losses. Moreover, their measurement showed that the energy savings of infrared heating over underfloor heating increased to almost 15% during intermittent operation with user-adaptive control, indicating that the control strategy has a significant effect on energy consumption. In a similar way, a Dutch performance assessment study [21] came to the conclusion that modulating the power of IR heater gives better comfort and reduces electrical peak stress compared with simple on/off control, and the study points out that IR heating might work well for small apartments or intermittently occupied dwellings because of their quick response and low installation requirements.

Beyond heating system configuration and control, an increasing amount of research addresses how surface properties affect radiative heat exchange and energy consumption. Heider et al. [17] also noticed that, while IR heating panels can increase a room's average surface temperature, most interior surfaces (excluding the surfaces of IR heating systems) stay colder than in rooms with underfloor heating. Hence, they mentioned that using low-emissivity surfaces, like wood or smooth concrete, perceived warmth can be increased without raising wall temperatures, as such surfaces reflect infrared radiation toward occupants. They concluded that IR reflective surfaces might improve the efficiency of IR heating systems and recommended further research in this field. This perspective is supported by later studies that emphasize the key role of surface emissivity in improving radiant efficiency.

Xu and Raman, through CFD simulations, demonstrated that dynamically adjusting the thermal emissivity of interior building surfaces can isolate the mean radiant temperature from wall and floor temperatures, which allows a reduction in the required air temperature setpoint to maintain thermal comfort [22]. They showed that, in cold weather, lowering surface emissivity to 0.1 allows a setpoint reduction of up to 6.5 °C without any other additional heat sources except the occupants themselves. However, this advantage becomes a penalty in summer by increasing cooling demand. The findings highlight the significant influence of emissivity on thermal comfort and heating efficiency. Through experimental work in a test cabin, Joudi et al. discovered that the use of reflective coatings on the interior and exterior walls reduces radiative heat exchange between wall surfaces and the environment, which lowers the heating

as well as the cooling energy demand [23]. Similarly, Malz et al. investigated IR reflective wall paints in existing buildings and discovered that they can reduce heat losses by as much as 22% while maintaining thermal comfort [24].

It is apparent from these findings that IR heating shows clear potential for optimization through improved dynamic control and by giving attention to surface emissivity. Although many studies have compared IR heating to conventional heating systems, there is limited research specifically exploring the combination of reflective interior walls with IR heating. Wille et al. [25] introduced infrared heaters combined with IR-reflective walls in a simulation study to raise the radiant temperature felt by occupants. This setup helps maintain thermal comfort at lower air temperatures by reflecting more heat back toward the occupants rather than being absorbed by the walls, ultimately resulting in energy savings.

Building upon their simulation study, Wille et al. (2025) [26] carried out controlled climate chamber experiments to assess the combined effects of IR heaters and IR reflective interior walls and showed a clear link between wall emissivity and occupant comfort, especially at higher IR heating powers. It was discovered that the Predicted Mean Vote (PMV) rises with decreasing wall emissivity, primarily due to the higher mean radiant temperature experienced by the occupant. This finding indicates the potential for energy savings through reduced air temperature setpoints when reflective walls are used in combination with IR heaters. Based on the measured data, the authors created a regression function PMV $= f(T_{\text{wall}}, T_{\text{air}}, \varepsilon, P_{\text{IR}})$, which can be employed as a control method to dynamically adjust IR heater output and to preserve the appropriate thermal comfort.

The findings from Wille et al. (2025) [26] clearly demonstrate the potential of combining IR heating systems with IR reflective interior surfaces to reduce heating energy demand while maintaining equivalent thermal comfort. However, their experiment was performed under controlled test chamber conditions, which do not fully represent the complex and dynamic behavior of actual building environments (e.g., heat transfer through walls). Moreover, the practical application of the proposed PMV regression model at the building scale remains unexplored. Therefore, this thesis extends the work of Wille et al. by implementing and evaluating a building model that simulates IR heating combined with IR reflective walls under realistic boundary circumstances.

1.3 Research objective and approach

The primary objective of this thesis is to quantify the energy saving potential of IR heating in combination with IR reflective interior walls at the building scale under realistic operating conditions. Specifically, the study aims to identify which combinations of weather types, occupancy patterns, and building insulation levels yield the greatest reductions in heating energy usage while maintaining thermal comfort within the acceptable standards. A further goal is to discover which of these configurations achieves the lowest GHG emissions and operational fuel costs.

In order to fulfill the research objective, this thesis investigates a hybrid heating strategy that combines a conventional base heating system with an occupant-activated infrared panel and infrared reflective interior walls. The analysis begins with a simple house model designed to isolate the direct radiant effects of the IR panel and reflective surfaces, where a conventional

system maintains a low baseline air temperature. The study is then extended to a standard reference hotel guestroom to examine the influence of adjacent zones and more realistic boundary conditions. The performance of the hybrid strategy is evaluated across various combinations, allowing the identification of operating conditions under which the system is most effective. The control of the IR panel is implemented using the PMV based regression function, integrated into EnergyPlus to dynamically modulate IR power output and maintain the desired comfort level while preventing unnecessary operation. Throughout the analysis, the work quantifies heating energy end use, greenhouse gas emissions, and operational fuel costs, and compares the hybrid strategy with conventional heating solutions, thereby bridging controlled test chamber insights with building scale performance under realistic operating conditions.

2. Theoretical Base

This chapter introduces the fundamental concepts required to understand the methods and analysis presented in this thesis. The discussion begins with the core principles of heat transfer, followed by an overview of radiative heat transfer and the characteristics of infrared heating. Further, the concept of thermal comfort is discussed, with emphasis on its relevance for space heating systems. The chapter concludes with a brief introduction to the EnergyPlus simulation tool and its modeling approach, providing the necessary context for the simulation work carried out in the remainder of this thesis.

2.1 Conduction and convection

There are three possible mechanisms for transferring heat: conduction, convection, and radiation. As described in the book by Modest [27], heat conduction in solids occurs because the atoms within a material are continuously vibrating. When a part becomes warmer, its atoms vibrate faster and transfer this extra energy to adjacent, slower vibrating atoms. This exchange continues from atom to atom, like a chain reaction through which thermal energy moves across the solid. For example, holding an ice cube makes our hands feel cold because heat is conducted from our hands to the ice cube. Fourier's law is mostly used to describe conduction as

$$q = -k\frac{\partial T}{\partial x}, \tag{2.1}$$

where q is the conductive heat flux, k is the thermal conductivity of the medium, x is the distance and T is temperature.

Convection, on the other hand, is the transfer of heat through the movement of a fluid such as air or water. Natural (free) convection happens when temperature differences create buoyancy that moves the fluid on its own because of density differences without external forces. Whereas forced convection occurs when an external force, such as a fan or pump, drives the fluid motion, which enhances heat transfer. (e.g., warm air rises and cold air sinks in a room with a convective heater, creating a circular flow). Thus, it is clear that both conduction and convection need a medium for energy transfer. The fundamental relationship for convective heat transfer is similar to heat transfer by conduction. Convective heat flux can typically be determined using a correlation such as

$$q = h\,(T - T_\infty), \tag{2.2}$$

where q is the convective heat flux, h is the convective heat transfer coefficient, T is the surface temperature, and T_∞ is the reference (ambient fluid) temperature. For the majority of applications, h and k do not have a strong influence of temperature. Convective and conductive heat transfer rates are therefore linearly proportional to temperature differences [27].

2.2 Radiation

In contrast to conduction and convection, radiation is transferred by electromagnetic waves or photons, which do not require a medium to travel [27]. One well-known example of radiation that spreads heat across the solar system is the radiation from the sun. Another key distinction between radiation and the mechanisms of conduction and convection is the reliance on temperature. Rates of radiative heat transfer are typically proportional to the fourth power of the absolute temperature. This behavior is explained by the fundamental radiation principles described in the following section.

2.2.1 Fundamental laws of radiation

There are several laws that describe how any object emits and absorbs thermal radiation, as well as the properties that influence the radiation heat transfer. The most relevant of these are outlined below.

Stefan-Boltzmann law

When determining the total radiant heat emitted by any object, the Stefan–Boltzmann law serves as the fundamental equation for calculating the total power radiated by a surface. It explains how the total radiative energy from a blackbody (an ideal surface that absorbs all incident radiation) rises rapidly with the fourth power of its absolute temperature. This can be noticed in the Figure 2.1, which represents the Stefan-Boltzmann law. The steep rise in the curve explains why hot surfaces, such as fires, emit far more radiant energy than cooler surfaces, even for relatively small temperature rises. This is due to the fourth power dependence on temperature. It means even a small increase in temperature will lead to a large increase in radiated power.

For actual surfaces, the law incorporates the emissivity factor ε, which accounts for the deviations from an ideal blackbody:

$$P = \varepsilon \, \sigma \, A \, T^4 \tag{2.3}$$

where
P: total emitted power (W),
ε: emissivity of the surface (dimensionless, $0 \leq \varepsilon \leq 1$),
σ: Stefan-Boltzmann constant ($5.67 \times 10^{-8}\,\mathrm{W\,m^{-2}\,K^{-4}}$),
A: surface area (m^2),
T: absolute temperature of the surface (K).

The emissivity represents the efficiency with which a material emits thermal radiation compared to a perfect blackbody ($\varepsilon = 1$). Typical values vary widely, for example, polished aluminum ($\varepsilon \approx 0.04$) and rough brick ($\varepsilon \approx 0.93$) [28].

The Stefan-Boltzmann law defines the total radiative energy emitted by a surface depending on its temperature. However, it does not describe the distribution of this energy over various wavelengths. Thus, the findings of Wien and Planck must be considered.

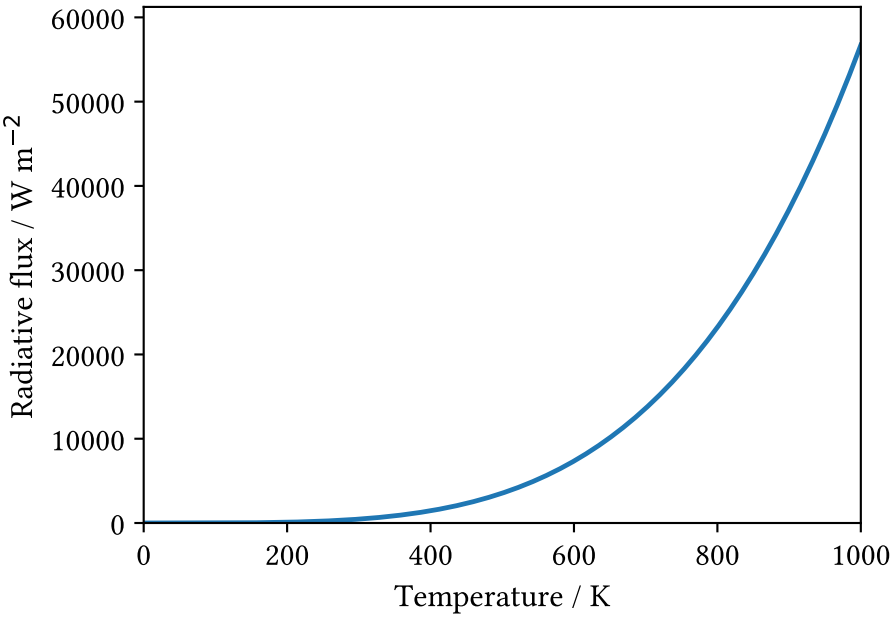

Figure 2.1: Radiative flux vs. temperature, showing $P \propto T^4$ based on [27]

Wien's displacement law

Wien found a relationship between the temperature of the blackbody and the wavelength at which the surface emits the maximum radiation. He discovered that as the temperature of a body increases, the wavelength corresponding to its maximum radiation intensity shifts toward shorter wavelengths.

$$\lambda_{\text{max}} = \frac{b}{T} \tag{2.4}$$

where
λ_{max}: wavelength of maximum spectral emission (m),
T: absolute temperature in kelvin (K),
b: Wien's displacement constant (2.897×10^{-3} m K).

The same can be expressed in a more generalized way:

$$\lambda_{\text{max}} \times T = 2.897 \times 10^{-3}\,\text{m K} \tag{2.5}$$

This relationship makes it simple to estimate the peak radiation intensity by knowing the temperature of the emitting body and vice versa. It tells that the hotter objects emit their peak radiation at shorter wavelengths. On the other hand, the cooler objects are at comparatively longer wavelengths. This explains why IR heaters peak in the infrared range, whereas the sun peaks in the visible region of the spectrum.

Planck's law

Planck's law explains the spectral nature of electromagnetic radiation emitted by a blackbody at a specific temperature. It illustrates how the emitted radiation is distributed across a range of

wavelengths for a given temperature and shows that all surfaces emit radiation at a variety of wavelengths and the temperature influences the intensity and peak of this radiation. Planck derived the following formula, which gives the spectral emissive power of a blackbody at absolute temperature:

$$E_\lambda(T) = \frac{2\pi hc^2}{\lambda^5} \frac{1}{\exp\left(\frac{hc}{\lambda kT}\right) - 1} \tag{2.6}$$

where
h: Planck's constant (6.626×10^{-34} J s),
c: speed of light in vacuum (2.998×10^{8} m s^{-1}),
k: Boltzmann's constant (1.381×10^{-23} J K^{-1}),
T: absolute temperature (K),
λ : wavelength (m).

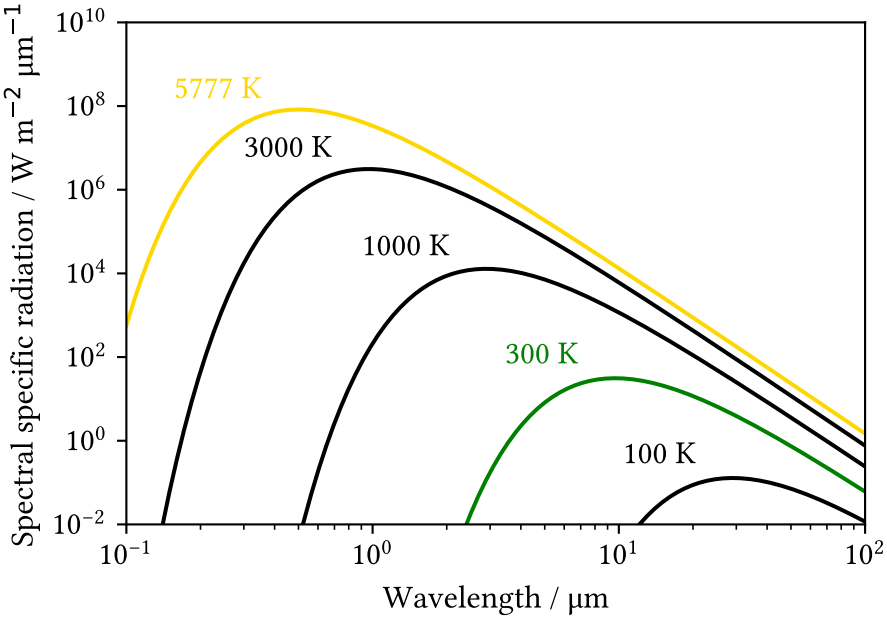

Figure 2.2: Spectral radiation vs. wavelength based on [29], the 300 K spectrum represents ambient temperatures on earth, whereas the 5777 K is the surface temperature of the sun

Figure 2.2 represents the spectral behavior of radiation at various temperatures. It shows that warmer surfaces display their peak radiation intensity at shorter wavelengths. Moreover, it tells that bodies with higher temperatures emit radiation with higher intensities. The same phenomenon is reflected in the Stefan–Boltzmann law, which basically is the integral of Planck's law over all wavelengths and therefore provides the total radiative heat flux emitted by a surface. At an ambient conditions with 300 K, a surface emits approximately 460 W m^{-2} of total radiation, whereas the surface of the Sun with 5777 K emits about 63 MW m^{-2}. This large difference illustrates the strong dependency of radiation on temperature.

Planck's law is especially significant considering infrared heating because it describes how surfaces radiate the majority of their energy in the infrared region of the electromagnetic spectrum at typical heater operating temperatures. As a result, Planck's law helps in determining the effective temperature and wavelength range that are important for designing and assessing infrared heating systems.

2.2.2 Radiative heat transfer

Energy is continuously exchanged between objects through radiation, originating from molecular and electronic oscillations on the surface. Once emitted, this energy travels in the form of electromagnetic waves [29]. When an electromagnetic wave emitted by one surface reaches another, its oscillating electric and magnetic fields interact with the charged particles within the atoms of the receiving surface. These interactions cause the atoms to vibrate more, increasing their internal energy and eventually their temperature. In this way, energy is transferred from one body to the other through electromagnetic waves, without requiring physical contact or any intervening medium [27]. Unlike conduction, where heat transfer solely follows a temperature gradient, radiative heat exchange takes place in both directions between surfaces. However, the net heat transfer always occurs from the warmer surface to the cooler one.

The interaction between emitting and absorbing surfaces through electromagnetic waves represents the fundamental mechanism of radiative energy transfer. An everyday example of radiative heat transfer, or thermal radiation, can be observed when we feel warmth from the sun's rays. Another instance occurs when a person stands near a fire, the side facing the fire feels much warmer than the side that is exposed to surrounding colder surfaces.

Characterization	**Wavelength**, λ	
Cosmic rays	< 0.3 pm	
Gamma rays	0.3–100 pm	
X-rays	0.01–30 nm	
Ultraviolet light	3–400 nm	
Visible light	0.4–0.7 µm	**Thermal Radiation**
Near infrared radiation	0.7–30 µm	**0.1–1000** µm
Far infrared radiation	30–1000 µm	
Millimeter waves	1–10 mm	
Microwaves	10–300 mm	
Shortwave radio & TV	300 mm–100 m	
Longwave radio	100 m–30 km	

Table 2.1: Forms of the electromagnetic wave spectrum based on [13]

The technical term electromagnetic wave may initially sound unusual. However, the general names for this kind of wave are quite familiar, such as visible light, radio waves, X-rays, infrared radiation, etc. They are primarily characterized by their wavelengths [27]. Table 2.1

shows the electromagnetic spectrum and illustrates how electromagnetic waves are classified according to their wavelengths.

Table 2.1 of the electromagnetic spectrum indicates that thermal radiation has a wider range of wavelengths, ranging from 0.1 µm to 1000 µm [13]. Infrared radiation has wavelengths greater than visible light yet shorter than microwaves. Human eyes cannot detect infrared radiation, however we can experience its effects as heat.

Radiative properties of surfaces

When thermal radiation hits a surface, some of the energy is absorbed, some is reflected, and a fraction may be transmitted for non-opaque materials [27]. As a result, the total incident energy is divided into three parts, and only the energy that is absorbed will heat the surface. The absorptivity α, reflectivity ρ, and transmissivity τ show the relative behavior of a surface that can be seen from Figure 2.3 and together satisfy the equation that is represented as:

$$\alpha + \rho + \tau = 1 \tag{2.7}$$

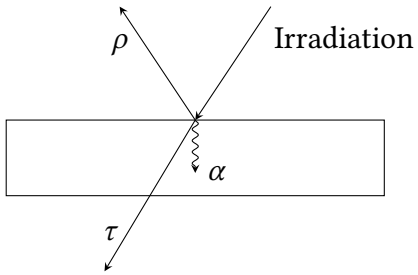

Figure 2.3: Schematic of incident radiation on a surface based on [27].

Since the transmissivity of an opaque body is very small ($\tau \approx 0$), $\alpha + \rho = 1$. The emissivity ε is defined as the fraction of energy a real surface emits compared to the theoretical maximum of an ideal blackbody ($\epsilon = 1$) at the same temperature. According to Kirchhoff's law of thermal radiation, for a surface in thermal equilibrium, the emissivity equals absorptivity. It further states that emittance is equal to absorptance at a given wavelength and a temperature [29]. Mathematically, this can be stated as:

$$\varepsilon_\lambda(T) = \alpha_\lambda(T) \tag{2.8}$$

This relationship means that a perfect emitter also serves as a perfect absorber, and vice versa. Therefore, highly reflecting materials with low absorptivity have low emissivity, whereas dark surfaces with high absorptivity are also highly efficient emitters. These properties are important when it comes to infrared heating because they affect how well surfaces absorb or emit radiant energy and influence how heat is distributed across an interior space. It should also be noted that, as these properties are wavelength dependent, a surface may appear visibly white but still can be a good IR emitter, such as a white IR panel heater.

Radiative heat exchange between two surfaces

The Stefan-Boltzmann equation measures the total radiative power emitted by the surface. However, it does not take into consideration the amount of this emitted energy that actually

reaches the other surface or is absorbed by it. In addition to the temperatures and surface properties of the bodies involved, radiative heat exchange between surfaces also depends on their geometry. This geometric relationship is defined as the fraction of the total radiation emitted by surface 1 that is intercepted by surface 2, this relationship is known as the view factor [29]. Basically, view factor describes how well one surface sees the other. This factor is influenced by their size, distance from one another, and orientation.

The net radiative heat exchange between two diffuse, gray surfaces (a surface that partially absorbs and partially reflects, $0 < \varepsilon < 1$) is calculated by the temperature difference between them, their emissivity, and the view factor given by the geometric arrangement. In practical applications, this relationship makes it possible to forecast how much radiant energy emitted by the heater surface effectively reaches and warms the surrounding surfaces. The following equation 2.9 describes the net radiative heat exchange rate between two surfaces, where the denominator represents the total radiative resistance between the two surfaces, including the effects of their emissivity and geometric configuration as stated in the textbook by Modest [27].

$$\dot{Q}_{12} = \frac{\sigma \left(T_1^4 - T_2^4\right)}{\frac{1-\varepsilon_1}{\varepsilon_1 A_1} + \frac{1}{A_1 F_{12}} + \frac{1-\varepsilon_2}{\varepsilon_2 A_2}} \tag{2.9}$$

where $\dot{Q}_{12}$ is the net radiative heat transfer rate from surface 1 to surface 2, A_1 and A_2 are the surface areas and F_{12} represents the view factor between two surfaces. This formulation is especially helpful, where the net heat transfer depends on both material characteristics and geometry, such as in infrared heating applications.

2.3 Infrared heating

In general, buildings are heated by radiation in a number of different ways. Solar radiation transmitted via windows is the most common source of radiant heating in buildings. Research indicates that south-facing windows can highly affect solar heat gains, thereby influencing the building's heating and cooling demands due to passive heating and increased solar radiation [30]. Moreover, internal heat sources continuously emit both radiant and convective energy, influencing the overall thermal balance [31]. Understanding the sources of radiation heating and the way building components influence these effects is vital for optimizing building design, lowering energy consumption, and increasing occupant comfort [32].

In this section, the practical application of thermal radiation in the form of infrared heating is introduced. To understand the behavior and performance of such heating systems, it is essential to examine their characteristic wavelengths, how they differ from conventional convective heating systems, and the resulting effects on indoor heat distribution.

Infrared spectrum

The International Commission on Illumination [33] and International Commission on Non-Ionizing Radiation Protection [34] have three subdivisions for the IR radiation as given in Table 2.2.

These three subdivisions, labeled as IR-A, IR-B, and IR-C, each serve distinct practical ap-

plications, progressing from shorter to longer wavelengths as one moves from IR-A to IR-C. Most residential infrared heating systems often function within the far-infrared spectrum (IR-C band) [35], as this wavelength range provides gentle radiant heat appropriate for indoor use. Because these wavelengths are longer than those of near and mid infrared, far infrared wavelengths have lower temperatures, as shown in Table 2.2 and thus lower energy intensity. With the help of Planck´s law and Wien's displacement law, this phenomenon can be justified. Because of lower energy intensity, domestic infrared heaters need a larger surface area.

Description	**Wavelength** (µm)	**Temperature according to Wien** (K)
Near infrared / IR-A	0.78–1.4	over 1600
Mid infrared / IR-B	1.4–3.0	800–1600
Far infrared / IR-C	3.0–1000	3–800

Table 2.2: Classification of infrared radiation

As discussed, far infrared radiation has longer wavelengths and lower intensity than near and mid infrared. This means that far infrared photons carry less energy due to their lower frequency. As a result, far infrared radiation is harmless to humans. In contrast, radiation such as ultraviolet, X-rays, and gamma rays consists of much higher energy photons that can damage DNA, which is why they are associated with serious health risks to humans.

The International Commission on Non-Ionizing Radiation Protection [34] confirms that, as far infrared radiation has long wavelengths and lower intensity than those of near and mid infrared, it penetrates only into the outermost layers of human skin. Therefore, the use of infrared heating in the household is considered safe and does not pose a hazard under regular exposure conditions.

Comparison with convection heating

In contrast to convection techniques, which mainly heat air [18, 16], radiation plays a crucial role in infrared heating because it allows direct heat transfer to surfaces [13], improving energy efficiency. In other words, heat radiates in waves, striking objects like people, walls, and furniture, where it is absorbed. Because of this direct transfer, infrared heaters can gradually retain heat by warming a building's thermal mass [14]. They slowly release the heat back into the space, resulting in a uniform and comfortable temperature distribution. As a result, IR heating has the potential to provide equivalent thermal comfort at a lower air temperature [22, 23, 20, 19, 25].

As described in Figure 2.4, the left side represents a conventional heating system, which mainly relies on convective heat transfer. This system causes air movement and circulation within the zone and needs longer times before the occupants feel comfortable and often demands a comparatively higher setpoint. In contrast to convective heating, infrared heating, shown on the right side, operates primarily through radiation and directly hits the objects and occupants. This way, it provides quick thermal comfort and therefore allows for a lower heating setpoint.

Moreover, to further enhance the effectiveness of IR heating, a new concept involving reflective

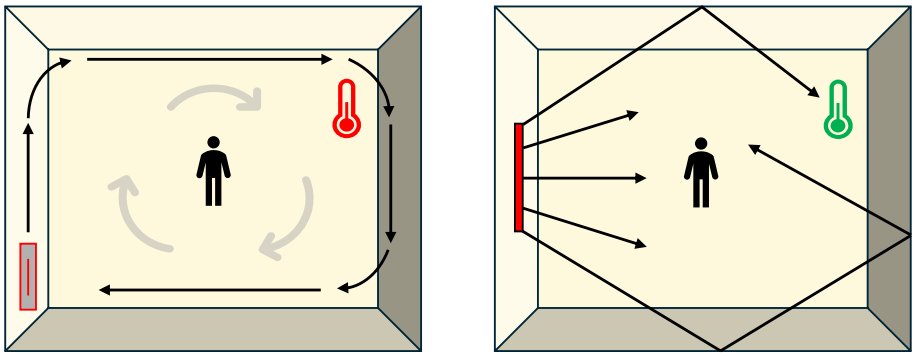

Figure 2.4: Convective vs. radiative heating

surfaces is being explored. With the addition of reflective walls, reflected infrared radiation can be redirected back into the room, enhancing the overall radiation temperature, which also reduces the heat losses through the walls, as the surfaces remain cooler because of their higher reflectivity. Several studies have demonstrated that the use of IR reflective walls improves heating performance and eventually leads to energy savings [24, 22, 25].

2.4 Thermal comfort

The primary goal of a heating system is to create an indoor thermal environment where occupants feel comfortable. This leads to the concept of thermal comfort, which is described by ISO 7730 [36] and ASHRAE standard 55 [37]. As per the definition of ASHRAE, thermal comfort is "a condition of mind that expresses satisfaction with the thermal environment". It means that under a comfortable thermal environment, the occupant feels neutral, neither too cool nor too warm. This condition or state needs to be expressed with some physical parameters in order to control the heating, ventilation, and air conditioning systems inside a building envelope according to the comfort requirements of an occupant.

2.4.1 Fanger's thermal comfort model

Among the various approaches used to define thermal comfort, Fanger's thermal comfort model [38] remains widely recognized and is an accepted theory that is standardized in ASHRAE standard 55 [37] and ISO 7730 [36]. According to Fanger's theory and the established thermal comfort standards, six key parameters influence an occupant's comfort. It includes air temperature, mean radiant temperature, metabolic rate (activity level), clothing insulation, air speed, and relative humidity. Based on a series of experimental studies, Fanger introduced the Predicted Mean Vote (PMV) index, which represents the average thermal sensation that a large group of occupants would report for any given combination of those six key parameters [38].

As shown in the Table 2.3, the PMV is evaluated on the standard seven-point thermal sensation scale, ranging from −3 (cold) to +3 (hot). As PMV does not directly indicate how many people are likely to feel uncomfortable, an index called Predicted Percentage Dissatisfied (PPD) is introduced.

The PPD gives the expected proportion of thermally dissatisfied occupants at a given PMV value [37]. Basically, it gives the percentage of people who would report thermally dissatisfied at a particular PMV value. Figure 2.5 describes the relation between PPD and PMV. As can be

PMV	Thermal Sensation
−3	Cold
−2	Cool
−1	Slightly cool
0	Neutral
+1	Slightly warm
+2	Warm
+3	Hot

Table 2.3: Sensation scale as per the PMV model based on [39]

seen that even at a PMV value of 0, there are 5% of people who are dissatisfied with the thermal conditions. This highlights that, despite standardized metrics, thermal comfort is ultimately a subjective and individual feeling of occupants.

ISO 7730 [36] recommends a PPD of less than 10% or PMV between −0.5 and +0.5 as an acceptable thermal comfort.

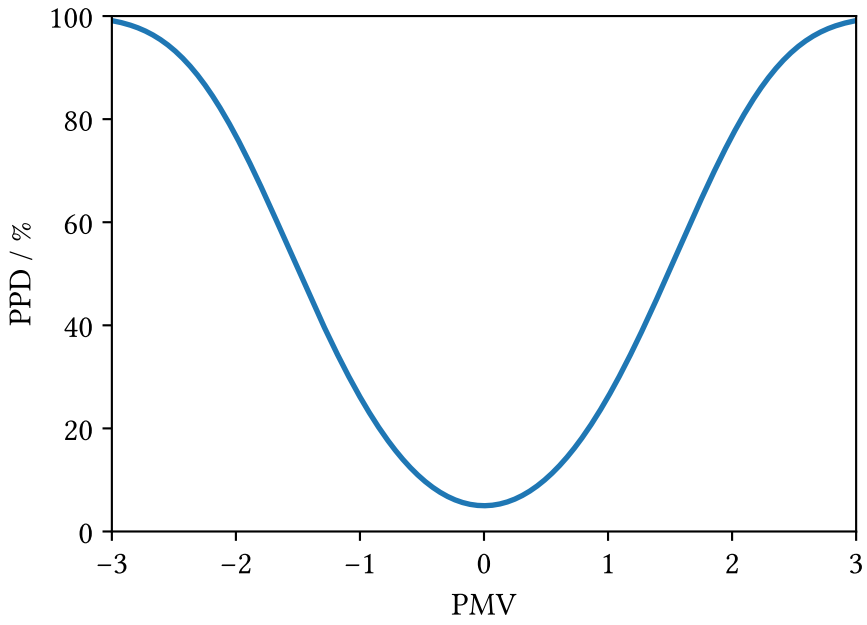

Figure 2.5: Relationship between PMV and PPD based on [39]

2.4.2 Radiant temperature asymmetry

As discussed, objects continuously exchange radiant heat with each other depending on their temperatures [29]. Consequently, human thermal comfort depends not only on air temperature but also on how the body exchanges heat with the surrounding surfaces. This interaction

is represented by the mean radiant temperature (MRT), one of the six parameters used in thermal comfort assessment. MRT represents the average temperature of all surfaces around an occupant, such as walls, windows, floors, and furniture, weighted by their emissivity and view factors relative to the occupants [37]. MRT plays a crucial role in determining thermal comfort, as humans gain or lose heat to the adjacent surfaces. Although the MRT offers an overall estimate of the surrounding radiative environment, it cannot detect situations where one surface is much warmer or colder than others, resulting in radiant temperature asymmetry.

According to Fanger et al. [40], radiant temperature asymmetry is the difference in the radiant temperature between two opposite sides of a small plane object. It occurs when different sides of the body are exposed to surfaces at significantly different temperatures. It means even if the overall mean radiant temperature or PMV is in the acceptable range, a large temperature difference around an occupant can create localized thermal discomfort. This phenomenon is especially relevant in infrared heating because it is primarily responsible for increasing radiant temperature [13]. Hence, if the system is not properly designed, IR heating might cause a large radiant temperature asymmetry. Both ASHRAE 55 [37] and ISO 7730 [36] standards define the acceptable limits of radiant temperature asymmetry. For example, asymmetry of up to 23 °C caused by a warm wall is acceptable as it results in approximately 5% of occupants who feel discomfort.

2.5 EnergyPlus

EnergyPlus is an open source building energy simulation tool developed by the U.S. Department of Energy [41]. It allows engineers and researchers to model the energy performance of a building under realistic operating conditions. The software can simulate heating, cooling, ventilation, lighting, plug loads, and water use, providing a comprehensive assessment of overall building performance. It includes detailed models for system components and uses advanced models to capture the dynamic interactions between the building, its HVAC systems, and the surrounding environment. These features enable EnergyPlus to provide a physically realistic estimate of real building performance.

2.5.1 EnergyPlus simulation interface

EnergyPlus provides a graphical interface called EP-Launch. It allows users to choose input files, start the simulation, and access output results through the interface. In order to perform an EnergyPlus simulation, two primary input files are required: the IDF (Input Data File) and the EPW (EnergyPlus Weather) file. The IDF defines all essential model information, including the building geometry, thermal zones, HVAC system configuration, internal gains, schedules, and control setpoints, whereas the EPW file provides the climatic data, such as temperature, humidity, and solar radiation, for the defined location. Figure 2.6 shows the EP-Launch interface, where the locations for selecting both the IDF and EPW files are visible.

Using these two files, simulations can be executed directly through the EP-Launch interface. Any modifications to the model can be made either using the IDF editor provided by EP-Launch or by editing the IDF directly in a text editor.

The lower section of the EP-Launch interface provides access to the simulation outputs. In the results section, tables are generated as html file and contain the complete set of outputs produced by EnergyPlus. In contrast, the variables explicitly requested by the user are collected

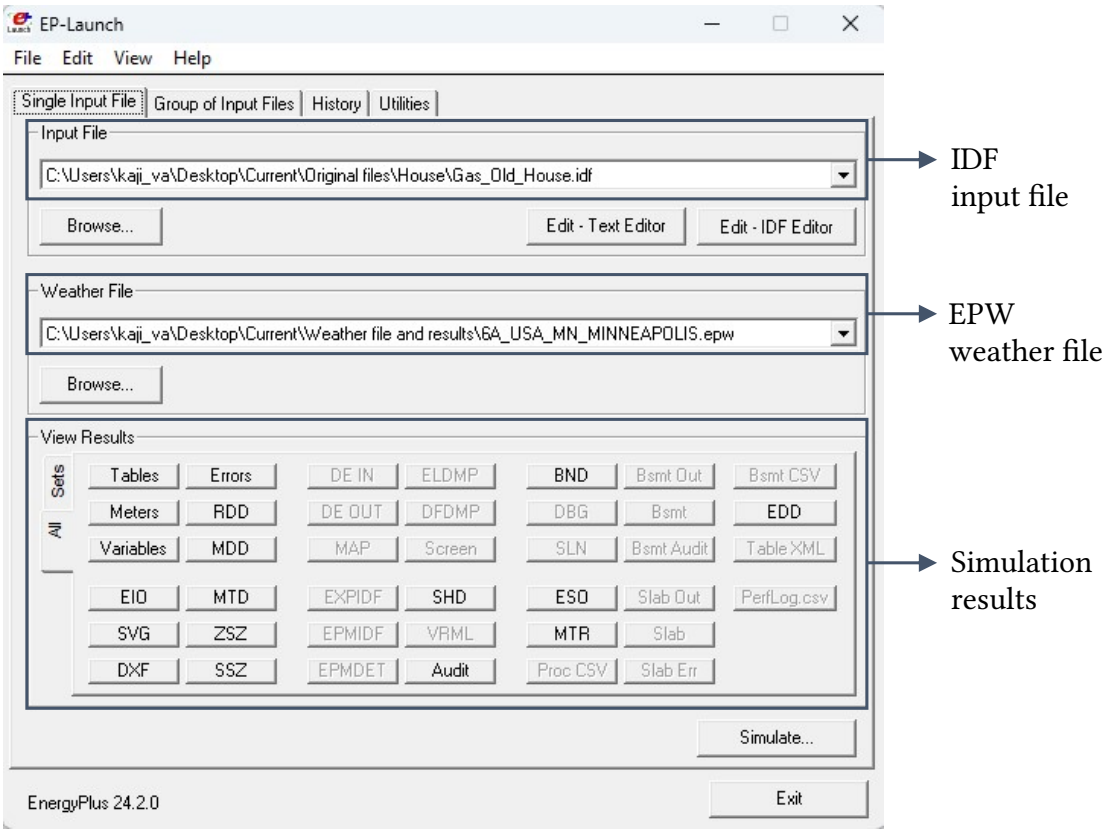

Figure 2.6: Screenshot of EP-Launch

in the variables section and exported as a csv file, containing only the selected outputs by the user. Additional sections for errors, warnings, and output diagnostics are also available.

2.5.2 Energy management system (EMS)

The conventional EnergyPlus objects alone are not sufficient to execute the dynamic control strategy required for this study. In order to modulate the infrared heater in real time, an additional layer of control logic is needed. Therefore, an energy management system (EMS) is used.

The EMS is an advanced feature of EnergyPlus that allows users to set up customized control strategies by overriding the selected aspects of EnergyPlus modeling. As described in the EMS application guide provided by EnergyPlus [42], a programming language called EnergyPlus runtime language (Erl) is used to define sensors, actuators, variables, and program logic. With EMS, it is possible to dynamically control equipment functioning within the EnergyPlus simulation. For example, turning HVAC systems on/off, adjusting output power, or employing occupant adaptive control logic. This flexibility enables the modeling of control approaches that are not available in typical EnergyPlus objects, making EMS particularly useful for research involving non-conventional strategies. Figure 2.7 explains the workflow of the EMS and shows how it controls the required variables.

EMS sensors: They provide a wide range of input data from the normal EnergyPlus output variables. They allow the controller to read zone or system-level quantities and to give the averaged or the summed output variables. In addition, schedule values exposed as output

variables can also be mapped to EMS sensors, making them available as inputs for custom control logic.

EMS program logic: The core of an EMS implementation is the control logic, which is written using Erl. Depending on the calling point, the EMS executes the user-defined logic to determine and apply the suitable control action.

EMS actuators: EMS actuators enable the Erl program to override or modify specific components of the EnergyPlus simulation during runtime. EMS can use these actuators to directly control selected model features, such as equipment power levels, system availability, or setpoint values. EnergyPlus provides a predefined collection of actuators for certain objects and components. However, not all equipment types support EMS actuation, and users cannot create custom actuators beyond those already accessible by the simulation engine.

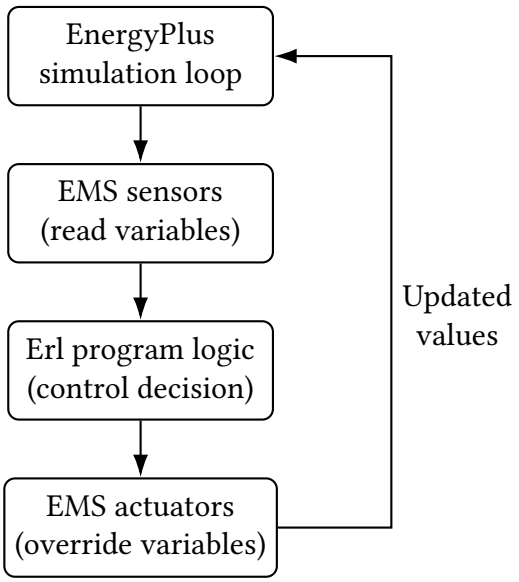

Figure 2.7: Schematic overview of EMS workflow

This entire workflow occurs at a particular EMS calling point, which defines when and where custom EMS programs are executed within the EnergyPlus simulation. These calling points indicate the particular stage of the simulation at which the EMS is allowed to interfere. A few examples of calling points include: at the end of zone sizing, during HVAC system iteration loops, or at the beginning of each timestep.

3. Simulation

This chapter presents the core simulation work carried out in this study. It begins with a detailed explanation of the broad methodology, followed by a description of the chosen reference buildings. Further, the various scenarios used to evaluate the proposed IR heating strategy are explained. Finally, the modeling of the heating systems and the implementation of the EMS inside EnergyPlus are outlined.

3.1 Methodology

The principal objective of this thesis is to quantify the energy and comfort implications of an infrared (IR) heating system combined with reflective interior walls, and to compare its performance with conventional heating systems. The hybrid strategy investigated here uses a conventional heating system to maintain a low baseline air temperature, while an IR heater provides radiant heating when occupants are present. The central hypothesis is that targeted radiant heating plus reflective surfaces can deliver equivalent thermal comfort at lower air temperatures, thereby reducing delivered heating energy, operating cost and CO_2 emission.

The overall research workflow and its key phases are summarized in Figure 3.1. The research employs a sequential approach beginning with a simplified single-room model to isolate the radiant heating effects of an IR heater combined with IR reflective wall surfaces, where a conventional convective heating system (e.g., gas boiler) maintains a low base air temperature and an occupant-activated IR panel delivers rapid thermal comfort. This controlled environment enables a clear assessment of direct surface and occupant heating, independent of complex whole-building interactions.

The analysis is then expanded to a U.S. Department of Energy´s prototypical small hotel guestroom. In doing so, the study evaluates how adjacent zone conditions influence the hybrid system's performance and overall effectiveness, with the primary goal of comparing the energy end use, operational fuel cost, and CO_2 emission associated with this new IR heating strategy against those of a conventional heating system in each context.

In addition to examining the influence of adjacent zones, the study evaluates how the envelope quality affects the new IR heating system by comparing two different building age models. Moreover, it assesses the performance of this proposed infrared heating system under diverse climatic conditions. The analysis is then further refined by considering different occupancy patterns, such as the living room with longer use and the dining room where occupancy is occasional and occupants primarily require quick thermal comfort for short durations only. This approach enables a comprehensive assessment of how both climate conditions and occupancy patterns impact the effectiveness and suitability of the proposed heating strategy in comparison to conventional systems.

The simulation and control of the IR heater in this study are based on a regression formula for the Predicted Mean Vote (PMV) derived by Wille et al. (2025) [26], who experimentally derived this relationship using IR heater and reflective walls inside a controlled test chamber. This regression function is implemented in this study to dynamically adjust the IR heater's power output. The energy management system (EMS) within EnergyPlus is utilized to implement this control logic, as described in detail in the following subchapters. Through this approach,

the IR heater is modulated to avoid unnecessary operation and to prevent both overheating and underheating, with the objective of maintaining occupant comfort as defined by a fixed PMV target within the regression function.

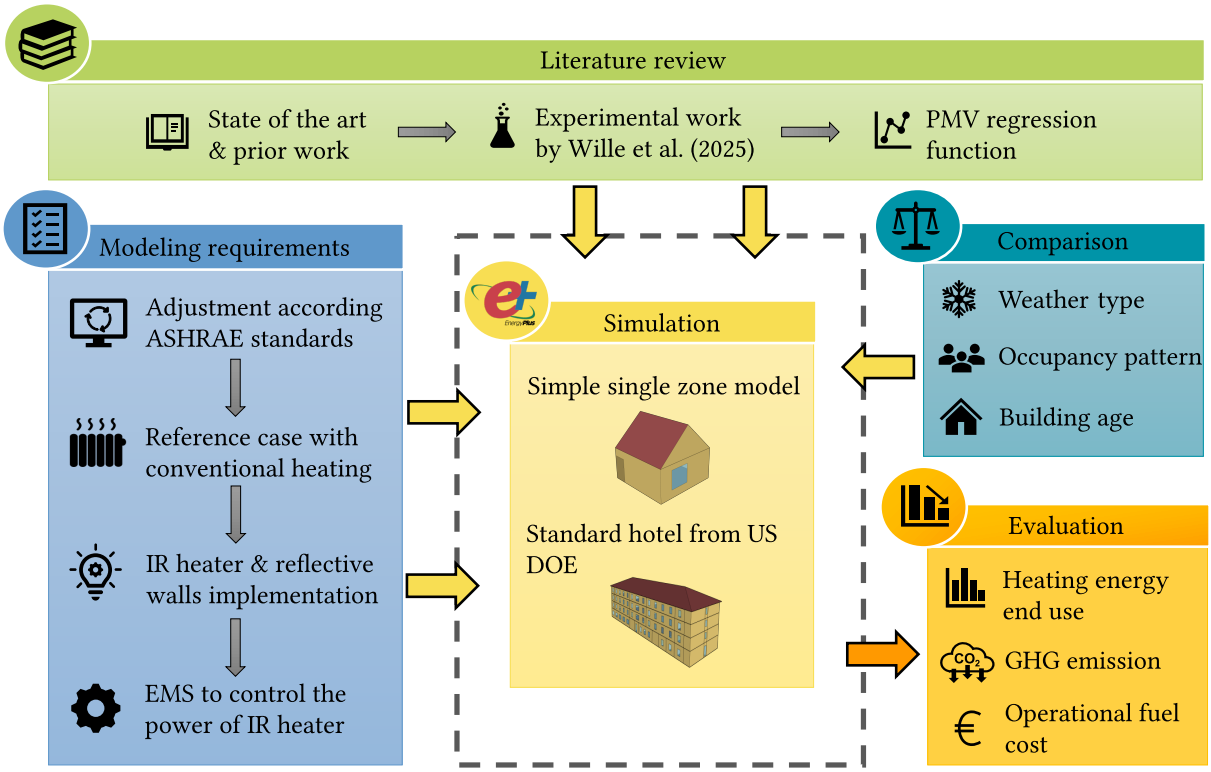

Figure 3.1: Research approach

3.2 Reference building

This study employs two different building models to evaluate the performance of the proposed heating strategy under varying conditions. Although the TABULA building typology [43] is frequently used for European residential building research, it was not selected for this study. TABULA very well provides standard building characteristics, such as building age, insulation level, and construction type, but it does not offer complete geometric descriptions or floor plans. For the current study, however, a defined and reproducible room geometry is essential to ensure that the results remain generalizable and applicable to a broad range of buildings.

3.2.1 Simple house model

The first model is a single zone house model that is used to isolate the direct radiant effect of the IR panel and reflective walls without the influence of adjacent spaces. This simple setup allows a clear interpretation of the fundamental heating behavior. The model titled *AirflowNetwork_Simple_House.idf* was adapted from example models developed by Energy Simulation Solutions Ltd. [44].

The adopted model was then adjusted to align with U.S. building reference standards, since the later analysis relies on the prototype building from the U.S. Department of Energy. Figure 3.2 shows the modified single zone model. The single zone geometry was defined with internal

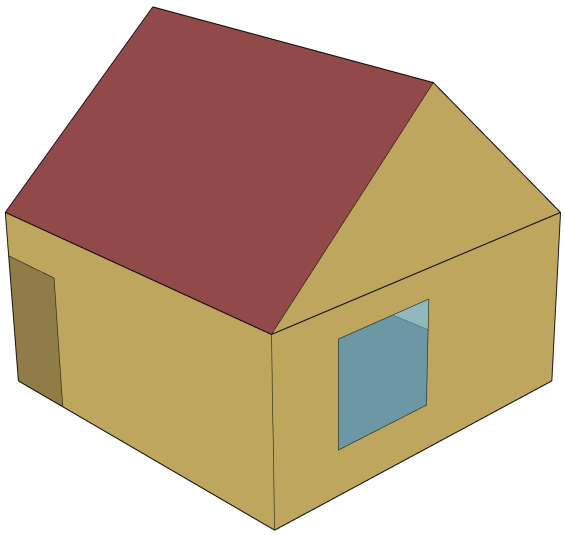

Figure 3.2: Simple house model

dimensions of 5 m × 5 m × 2.4 m. The zone has two windows, one on the east and one on the west. Since all four walls in this model are exterior walls directly exposed to the outdoor air, it represents a free-standing or detached house.

All internal gains, including plug loads, lighting, and occupants, are assigned according to the relevant standards and are summarized in the accompanying Table 3.1. Infiltration and ventilation rates are likewise defined following the same standard specifications.

The lighting power density was taken from the International Energy Conservation Code (2021) [45], which specifies a value of 5.38 W/m^2 for living spaces.

For the internal heat gains from occupants, the same metabolic activity level reported in Wille et al. (2025) [26] was used. In the experiment, this corresponds to a heat gain of 122 W per person based on a body surface area of 1.52 m^2. However, in EnergyPlus, occupants are represented with a larger surface area of 1.8 m^2, which leads to a heat gain of 144 W per person when applying the same metabolic heat generation of 80 W/m^2.

Internal gains	**Power**	**Standard followed**
Lighting	5.38 W/m^2	IECC 2021
Equipment	9.34 W/m^2	NREL 2022
People	144 W	Based on experiment

Table 3.1: Assigned internal gains in the house model

For the equipment power density, data from the End-Use Load Profiles for the U.S. Building Stock (National Renewable Energy Laboratory, 2022) [46] was used. The report provides a regression function for plug loads as a function of the number of occupants and the finished floor area (FFA). For single-family detached homes, the regression is given by

$$P_{\text{plug}} = 1146.95 + 296.94\, n_{\text{occupants}} + 0.30\ \text{FFA}.$$

In this study, a total of $n_{\text{occupants}} = 2$ is considered, and the floor area of the model is $25\,\text{m}^2$. Using the regression above, the resulting equipment power density is $9.34\,\text{W/m}^2$.

The required mechanical ventilation rate was determined according to the ASHRAE Handbook—Fundamentals (2017) [47], which refers to the residential ventilation requirements of ASHRAE Standard 62.2. The standard specifies the minimum whole-building ventilation rate as

$$Q_v = 0.15 A_{\text{cf}} + 3.5\,(N_{\text{br}} + 1)\,,$$

where Q_v is the required ventilation flow rate in L/s, A_{cf} is the conditioned floor area in m^2, and N_{br} is the number of bedrooms (with a minimum value of 1).

For this model, the conditioned floor area is $A_{\text{cf}} = 25\,\text{m}^2$ and, since the building has only one heated zone, the number of bedrooms is taken as $N_{\text{br}} = 1$. Substituting these values gives

$$\begin{aligned} Q_v &= 0.15\,\text{L}\,\text{s}^{-1}\,\text{m}^{-2} \times 25\,\text{m}^2 + 3.5\,\text{L}\,\text{s}^{-1} \times (1+1) = 3.75\,\text{L}\,\text{s}^{-1} + 7.00\,\text{L}\,\text{s}^{-1} \\ &= 10.75\,\text{L}\,\text{s}^{-1} \approx 0.0108\,\text{m}^3\,\text{s}^{-1} \end{aligned}$$

Infiltration represents the unintended leakage of outdoor air through the building envelope, which contributes to the heating load. The infiltration rate for this study is based on the guidance provided by the Air Conditioning Contractors of America in their document Infiltration Guidance for Buildings at Design Conditions (2022) [48]. The report provides recommended air change rates (ACH) for various building leakage categories. For this model, the semi-loose category is selected, which corresponds to an average air change rate of

$$\text{ACH} = 0.80\,\text{h}^{-1}$$

The infiltration volumetric flow rate is calculated using

$$Q_{\text{inf}} = \frac{\text{ACH} \times V}{3600},$$

where V is the volume of the space in m^3. The zone volume is computed from the floor area and ceiling height as

$$V = 25\,\text{m}^2 \times 2.4\,\text{m} = 60\,\text{m}^3.$$

Substituting the values gives

$$Q_{\text{inf}} = \frac{0.80 \times 60\,\text{m}^3}{3600\,\text{s}} = 0.0133\,\text{m}^3/\text{s}.$$

3.2.2 Hotel guestroom model

The other model considered in this study is the standard reference building provided by the U.S. Department of Energy (U.S. DOE) [49]. The U.S. DOE offers a set of prototypical building models for energy simulation research, and in this work, the small hotel reference building is used. Such standardized models help generate generalizable outcomes that can be applied to a broad range of building types. The model of the building is shown in Figure 3.3. It is a four-story hotel consisting of 74 rooms.

As discussed, the TABULA database [43] was initially considered because it is well suited for European residential buildings. However, TABULA does not provide detailed floor plans or the necessary geometric information required for building energy simulations. Therefore, the U.S. DOE reference building models were selected instead. Another reason behind selecting this building model is that previous researchers Xu and Raman [22] used the same U.S. DOE small hotel model in their analysis of energy savings achieved through modified surface emissivity. Using the same reference model, therefore provides continuity with the previous research.

In order to maintain the analysis focused and computationally manageable, only one representative guestroom is considered rather than analyzing all rooms. In contrast to the isolated single zone model, this room experiences heat transfer from adjacent heated guestrooms, making it more realistic.

The selected zone, highlighted in light green in Figure 3.3, corresponds to guestroom 214 with a floor area of 32 m^2. It has one exterior wall with a window, while the floor, ceiling, and one side wall are adjacent to conditioned rooms. The other two walls are connected to a stairwell and a corridor, respectively. This layout provides a more realistic boundary condition and allows the study of how adjacent zones influence the performance of the proposed heating strategy.

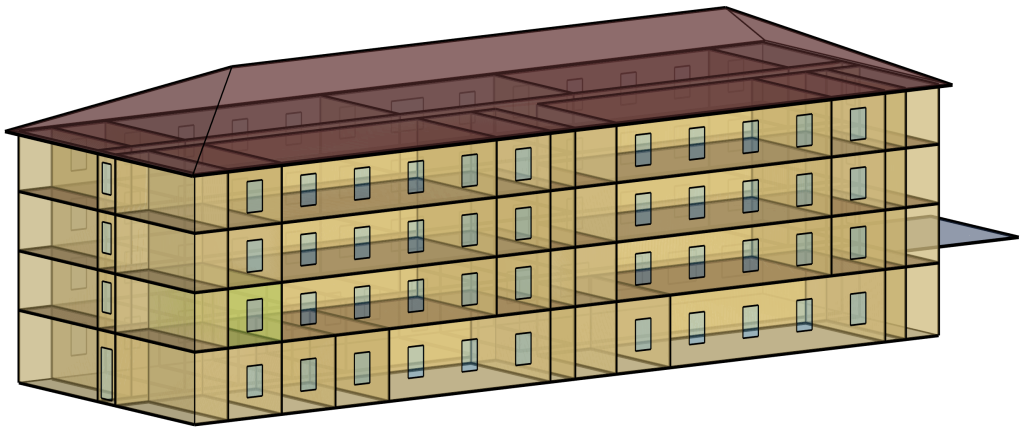

Figure 3.3: Standard small hotel building layout, highlighting the analyzed guestroom 214 in light green on the left side of the first floor

Because the DOE prototype is a standardized model, most of its characteristics were retained. Only the internal gains were adjusted as per the modern standards. The original model used outdated ASHRAE values, which reflected older lighting and equipment technologies. These were updated to current ASHRAE standards [50], accounting for modern systems such as LED lighting. Provided Table 3.2 explains the updated gains values compared to the original values.

Internal gains	**Original model (W/m^2)**	**Revised standard (W/m^2)**
Lighting	18.70	4.40
Equipment	14.30	11.84

Table 3.2: Revised internal gains

3.3 Different scenarios

In this section, the different simulation scenarios are presented, which are considered for evaluating the proposed heating strategy. Exploring several conditions makes it possible to examine how the system responds under varying boundary conditions and to identify which combinations of building insulation, weather type, and occupancy pattern settings yield the best performance. These scenario based comparisons allow for a systematic assessment of when and where this new IR heating approach is most effective relative to conventional heating systems.

3.3.1 Building age

The first scenario compares buildings of different construction ages. The purpose of this comparison is to look at how insulation quality influences the performance of the new heating strategy, since older buildings typically have poorer thermal insulation, while modern constructions usually feature better envelope performance. For both the old and new building models, the emphasis in this scenario is therefore placed on evaluating the impact of envelope quality and insulation level on heating demand and overall system behavior.

To ensure that the analysis remains aligned with building standards and yields generalizable results, two construction vintages from the U.S. DOE reference buildings are selected to represent an "old" and "new" building case. The DOE provides the reference building models for various construction periods. In this study, the pre-1980 and post-2004 models are used to account for poorly and well-insulated buildings, respectively. The corresponding thermal transmittance (U-value) for the envelope components of both models are summarized in the Table 3.3 and 3.4 below. For windows, the solar heat gain coefficient (SHGC) is also an essential parameter to be considered.

Construction	U-value (W/m^2K)
External wall	0.82
Roof	0.33
Floor	1.85
Window	3.53 / 0.41 (SHGC)

Table 3.3: Pre-1980 standard model

Construction	U-value (W/m^2K)
External wall	0.36
Roof	0.35
Floor	1.85
Window	3.24 / 0.39 (SHGC)

Table 3.4: New-2004 standard model

As shown in the tables above, the greatest improvement between the two construction standards is found in the external wall assembly, whose thermal transmittance decreases noticeably in the 2004 model. To achieve the improved performance, insulation thickness in the model is increased by 7 cm. In contrast, the roof, floor, and windows exhibit only minor changes in their thermal properties. Another noteworthy difference is the infiltration rate, which is reduced by 73% in the new model, representing a significant enhancement in envelope air tightness. These two modifications are the primary changes relevant to the analysis conducted in this study.

After determining the old and new envelope configurations, the respective U-values were applied to the single zone model to represent its “old” and “new” variants. This ensures that the simplified model uses envelope characteristics consistent with the U.S. DOE construction standards. In contrast, the second small hotel reference model already incorporates these standardized U-values, as it is directly based on the official U.S. DOE prototype. Therefore, no modifications to the envelope details were necessary for the hotel model. As a result, both models have comparable envelope characteristics in their respective old and new versions.

3.3.2 Occupancy pattern

The second comparison scenario examines different occupancy patterns. Understanding which type of occupancy schedule is most compatible with the proposed heating strategy is essential, especially since the literature suggests that infrared heating performs best during intermittent occupancy periods. To evaluate this claim, two representative occupancy types are considered. The first is a typical living room occupancy pattern, which reflects frequent and longer presence. The second is a dining room occupancy pattern, representing a short and occasional occupancy profile.

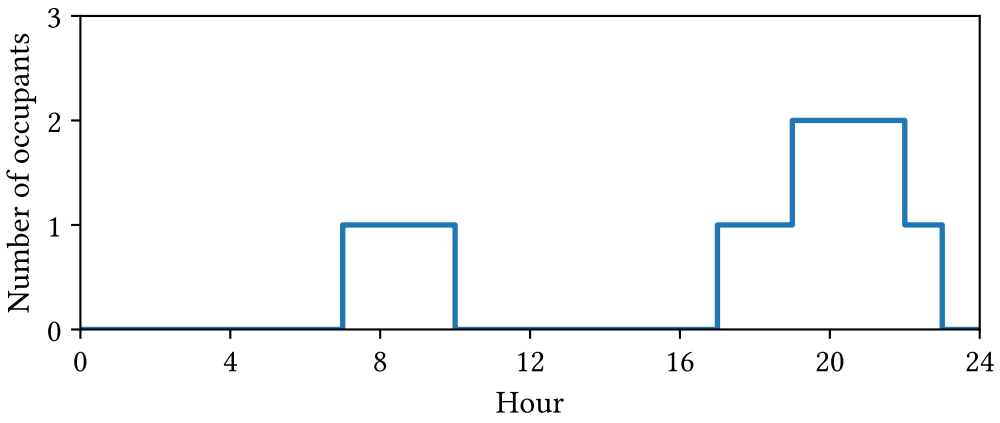

Figure 3.4: Living room occupancy schedule

The living room occupancy schedule is taken from the Prototype Residential Buildings for Energy and Sustainability Assessment developed by the National Institute of Standards and Technology [51]. This dataset provides occupancy in fractional form. However, since the purpose of this study is to activate the heater only when a full occupant is inside the zone, the fractional values are rounded to represent full occupant presence. Therefore, occupancy changes occur only at full hours, since the profile is defined on an hourly basis. Given Figure 3.4 shows the living room occupancy schedule.

However, no standardized schedule for dining room occupancy could be found in the literature. Therefore, the dining room pattern is assumed based on typical breakfast, lunch, and dinner periods to reflect realistic short-term use. That can be seen from the Figure 3.5 below.

These two occupancy profiles show different usage scenarios and allow an evaluation of which profile is better suited to the new IR heating system. Comparing these profiles also helps to assess how occupancy-driven control strategies influence energy savings and system efficiency.

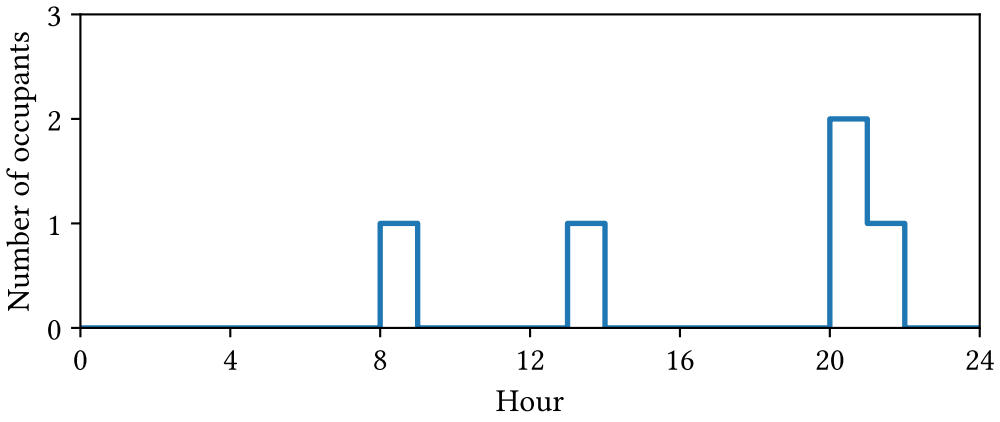

Figure 3.5: Dining room occupancy schedule

3.3.3 Climate type

A third key comparison in this study is based on weather type, examining how different climatic conditions influence the effectiveness of the proposed heating strategy. To capture a wide range of climatic conditions, two contrasting locations are selected. Minneapolis represents a continental climate with large seasonal temperature swings and severe, prolonged winters, while Stuttgart reflects a maritime climate with relatively mild winter conditions.

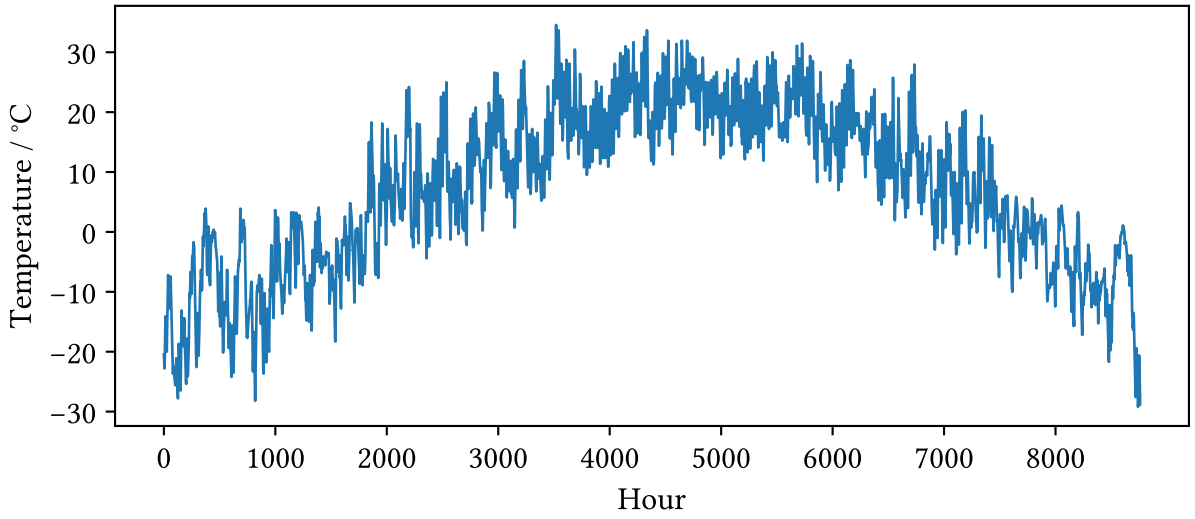

Figure 3.6: Dry-bulb air temperature in Minneapolis starting from January

The aim of this comparison is to determine under which climatic conditions the system achieves the highest energy savings.

The climatic profile of Minneapolis is illustrated in Figure 3.6. As can be seen, there is a noticeable difference between summer and winter weather in the city, with significant temperature swings and particularly harsh winters. The corresponding minimum and average outdoor temperatures are summarized in Table 3.5.

In contrast, Figure 3.7 illustrates the climatic profile of Stuttgart. As shown, the temperature variation throughout the year is comparatively moderate, with smaller differences between summer and winter conditions and overall milder winters than those observed in Minneapolis.

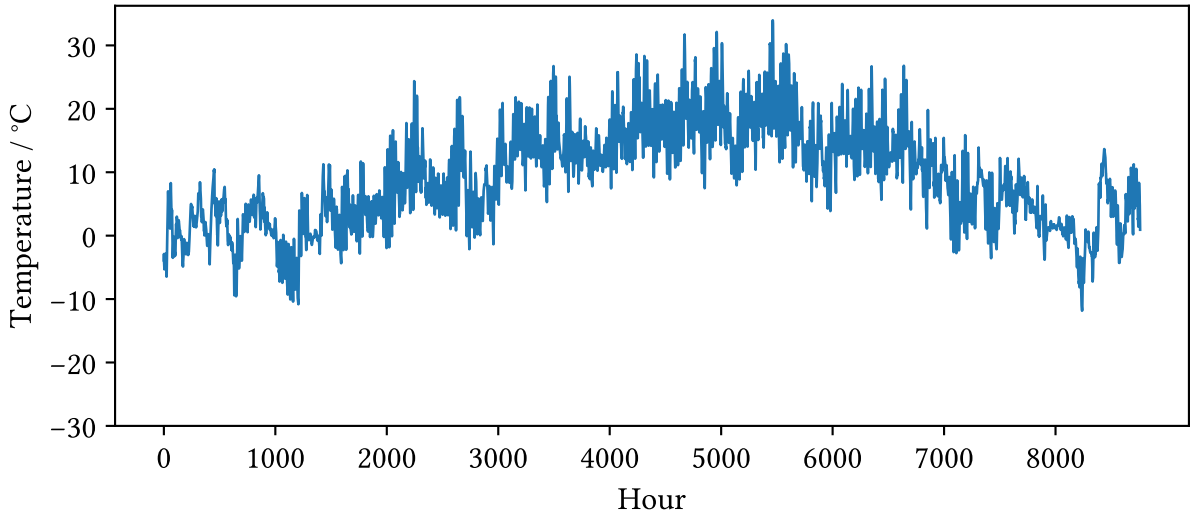

Figure 3.7: Dry-bulb air temperature in Stuttgart starting from January

Table 3.5 highlights the lowest and average winter temperatures for both locations, highlighting the substantial climatic differences between the two. Minneapolis reaches a minimum temperature of −29.2 °C, whereas Stuttgart experiences significantly a milder minimum of around −11.8 °C. These contrasting conditions provide a useful basis for evaluating the proposed heating strategy, allowing the study to examine how well the IR heating system performs under harsh versus mild winter climates and to determine which climatic condition offers the greatest potential for energy savings.

Location	**Lowest temperature (°C)**	**Average winter temperature (°C)**
Minneapolis	−29.2	−2.9
Stuttgart	−11.8	3.6

Table 3.5: Weather comparison

3.4 Modeling in EnergyPlus

This section describes the implementation of modeling elements and system configurations carried out in EnergyPlus using the Input Data File (IDF) and EP-Launch. The first part presents the setup of the heating systems, including their operational schedules, setpoint definitions, and component specifications. The second part details the implementation of the Energy Management System (EMS), explaining how custom control logic, sensors, and actuators are integrated into the EnergyPlus simulation environment.

To better understand the overall modeling approach, it is important to first visualize how each heating system works. The operational behavior of both heating systems is illustrated in Figure 3.8. On the left, the conventional system with gas heating and a convector heater can be seen, which primarily warms the space through convective heat transfer, maintaining a constant setpoint temperature of 21 °C.

In contrast, the right hand side shows the proposed IR heating approach, which combines a gas heater with an infrared panel and reflective walls. In this setup, the gas heater maintains a lower base air temperature of 18 °C, while the IR panel is activated only when the room is occupied. The IR panel rapidly delivers thermal comfort by directly warming the occupant and nearby surfaces. This effect is further enhanced by the reflective walls shown in the figure. Because comfort is provided through radiation rather than by heating the entire air volume, acceptable comfort conditions can be achieved at these lower air temperatures.

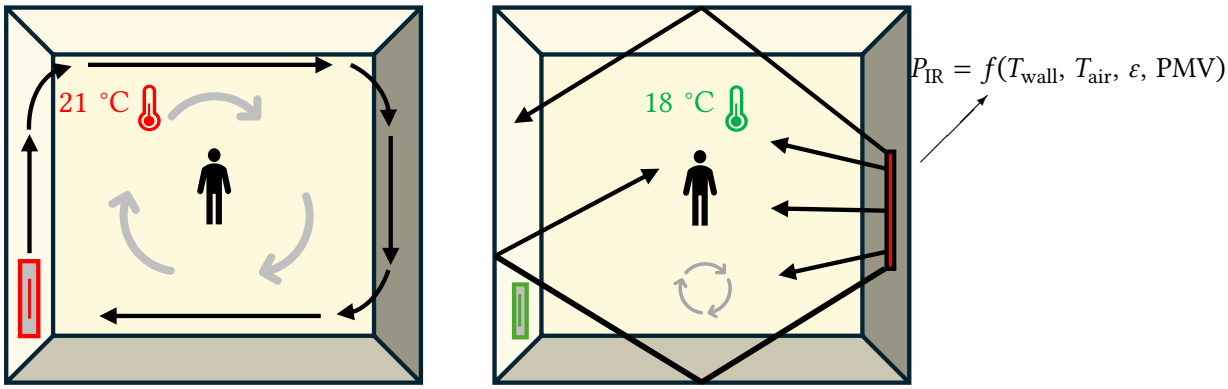

Figure 3.8: Working of new heating strategy compared to the conventional heating

Additionally, the power output of the IR heater is controlled using the PMV regression model developed from the experimental work of Wille et al. (2025) [26], ensuring that the IR heating responds precisely to the comfort needs of the occupant.

The modeling of these components is described in the following sections to make both heating systems operate as intended. Only the essential and relevant elements required to understand the functioning of the heating systems are discussed. Aspects such as building surfaces, material properties, constructions, and schedules are not included here.

3.4.1 Heating systems

This subsection describes the modeling approach for both heating systems within EnergyPlus and later also outlines how their annual on/off operation schedules were implemented.

Gas boiler

As the first step in the implementation, the gas heating system was modeled to serve as the baseline case. A *Coil:Heating:Fuel* object using natural gas was selected to represent a conventional gas boiler. The boiler efficiency was set to 80%, consistent with values reported in the literature [52]. The nominal heating capacity of the boiler was left on autosize, meaning that EnergyPlus determines the required capacity based on the building loads. In practice, this configuration represents an idealized boiler, capable of modulating its output to meet the heating demand at any timestep.

The boiler is assigned an "always-on" availability schedule. However, its operation is ultimately governed by the zone thermostat. For the baseline case, in which space heating is provided solely by the gas boiler, the heating setpoint temperature is fixed at 21 °C. However, for the new heating case, the setpoint temperature is reduced to 18 °C, since the IR heating directly compensates for the lower air temperature. Under this configuration, the gas system only activates when the zone temperature falls below these threshold values. With the autosized capacity and thermostat control, the boiler continuously adjusts its output to maintain the prescribed indoor temperature, ensuring stable operation throughout the simulation.

Infrared heater

To implement the proposed IR heating strategy, the first step was to model the infrared heater. EnergyPlus offers multiple dedicated radiant heating objects specifically designed to simulate infrared and radiant panel systems. Initially, these standard radiant heater models were used to represent the IR unit. However, during the EMS development phase, it became apparent that these radiant heater objects do not provide the required actuator interfaces for EMS control. Since the objective of this study is to dynamically modulate the IR heater power using EMS, the lack of EMS compatibility made these models inappropriate. The different radiant heating models that were initially used for representing the IR heater in this study are summarized in an Appendix A-1 that indicates that none of the models can be controlled through EMS.

Therefore, an alternative modeling approach was required, one that allows full EMS control while still representing the predominantly radiant behavior of an IR heater. The solution was to model the IR heater using the *ElectricEquipment* object, which functions as a controllable electric plug load whose power input can be overridden through an EMS actuator. Importantly, this object allows the user to prescribe the radiant, convective, and latent fractions of the emitted heat. To realistically approximate a domestic infrared panel, the radiant fraction is set to 0.70, consistent with values reported for typical residential IR heaters [53]. This configuration ensures that the equipment behaves as a high radiant heating device while providing full EMS compatibility for power modulation.

A screenshot of the implemented IR heater model in the IDF Editor is shown in Figure 3.9. As illustrated, it is implemented inside *GuestRoom214* and the *Fraction Radiant* parameter is set to 0.7. Another important parameter is the *Design Level*, representing the maximum heating power of the IR panel. This value was selected and scaled accordingly based on the experimental configuration used by Wille et al. (2025) [26], where the maximum employed IR power was approximately 600 W.

Because the hotel guestroom in this study has nearly twice the floor area, the design power was scaled to 1200 W to achieve a comparable radiant intensity. For the smaller single zone model, a design level of 900 W was chosen. Hence, the panel capacities used in both cases originate from experimental values and are proportionally adjusted according to the floor area of the respective zones.

Reflective walls

The next step in implementing the proposed heating strategy is to make the room surfaces infrared reflective so that more radiant energy is redirected back into the space. According to Kirchhoff's law of thermal radiation, a surface with lower emissivity also exhibits lower absorptivity, and therefore reflects a greater portion of incident infrared radiation. To achieve

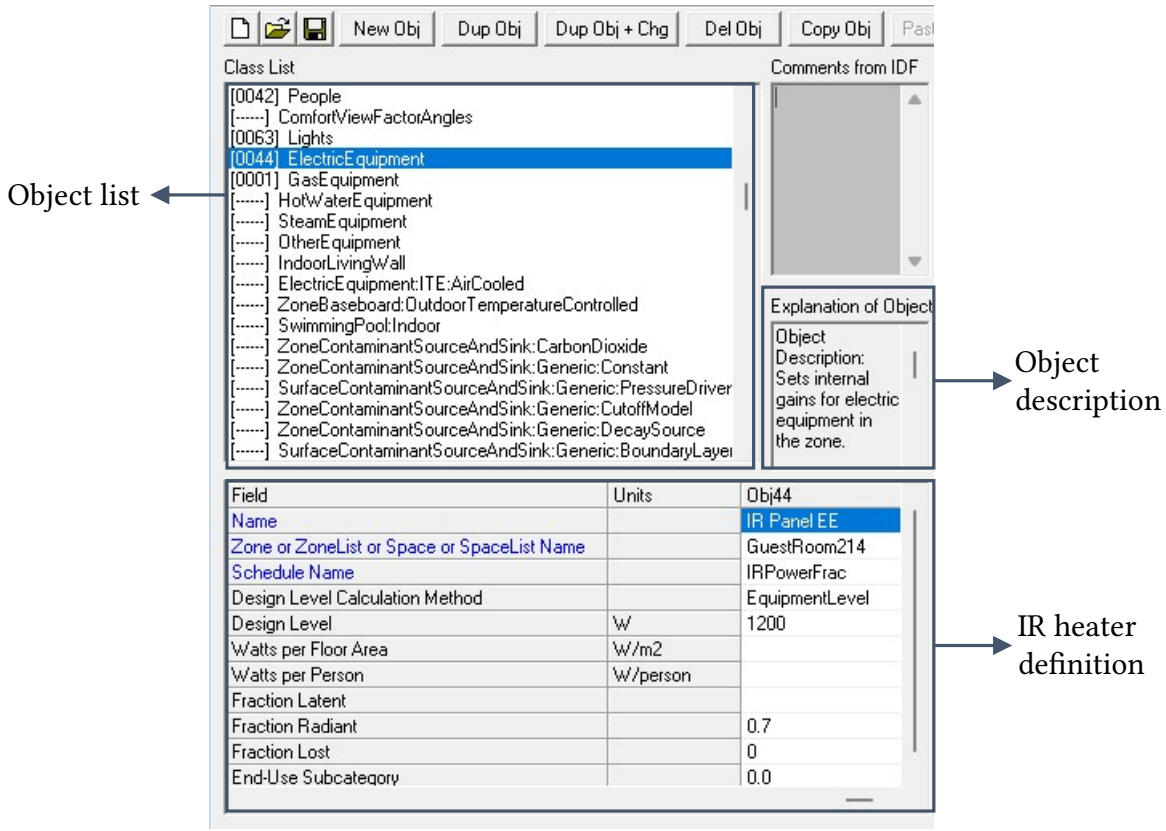

Figure 3.9: Screenshot of IR heater model from EP-Launch

this reflective behavior in EnergyPlus, the thermal absorptance of the wall materials was reduced.

In the standard construction, the exterior surface layer typically has an absorptance of 0.9. For this study, the value was reduced to 0.5. Selecting this intermediate value ensures that the simulation represents the core behavior within the experimental "Design of Experiment" rather than an extreme condition (e.g., $\varepsilon = 0.1$). Using $\varepsilon = 0.5$ provides a balanced and representative case that aligns well with the experiment and yields more promising results.

Schedule of heating systems

The scheduling of heating systems determines when the heating is turned on or off throughout the year. It is common to completely switch off space heating during the summer time when outdoor air temperatures are consistently high. The same principle is applied in this research.

Instead of selecting a random calendar date, a moving-average method is used to decide the start and end time of the heating season. A floating average of the outside air temperature over the last three days is calculated. If these three days float-average rises above 15 °C at the end of winter, the heating system is turned off. Conversely, when the same moving-average temperature drops below 15 °C in autumn, the heating system is switched on again.

Overall, the heating system remains off during the intermediate period (usually summer), and the start/stop dates of the heating season are set using this moving-average method to better reflect the actual building operations.

3.4.2 EMS

This section describes the implementation of the Energy Management System (EMS) in EnergyPlus, whose purpose is to dynamically adjust the power of the infrared heater. The objective of the EMS control is to activate the IR heater immediately when an occupant enters the zone and to provide quick thermal comfort. Thermal comfort is quantified using the Predicted Mean Vote (PMV), and the heater output is continuously adjusted based on the PMV requirement. The relationship between PMV and heater power is based on the regression function developed by Wille et al. (2025) [26] through controlled chamber experiments. This regression model serves as the core control logic for determining the IR heater's power level within each simulation time step.

EMS sensors

As outlined in Chapter 2, the first step in implementing a custom control strategy is to define the required sensors. Accordingly, several EMS sensors were defined to supply the real time input data needed by the control algorithm. These sensors monitor key environmental and comfort related variables inside the thermal zone, including air temperature, surface temperatures of the surrounding walls, floor, and ceiling, the current PMV value from the Fanger model, and the number of occupants present. Together, these variables allow the EMS to characterise the zone state and make appropriate control decisions for the infrared heater.

As an illustration, the following code snippet shows the EMS sensor used to read the zone air temperature:

```
EnergyManagementSystem:Sensor,
  ZoneTAir,                     !- Name
  GuestRoom214,                 !- Output:Meter Index Key Name
  Zone Mean Air Temperature;    !- Output:Variable
```

For each time step, this sensor provides the zone air temperature, which is then used both for determining the baseline PMV and for evaluating the regression based heating demand. For the remaining required variables, similar EMS sensors were defined.

EMS actuators

After defining the sensors, the next essential step in setting up an EMS is to specify the actuators. Actuators enable the EMS program to override selected variables within the simulation and apply the control actions determined by the custom logic. In this study, only two actuators were required: one for controlling the infrared heater power and one for adjusting the heating setpoint schedule.

The key actuator is the one linked to the IR heater. Through this actuator, the EMS writes a power fraction value between 0 and 1 to the control schedule, allowing the IR heater output to be modulated based on occupancy and the PMV based regression function. This actuator forms the core of the proposed heating strategy, as it enables real time adjustment of IR heating power. A code snippet of the IR heater actuator definition is shown below.

```
EnergyManagementSystem:Actuator,
    IRPowerActuator,      !- Name
    IRPowerFrac,          !- Actuated Component Unique Name
    Schedule:Compact,     !- Actuated Component Type
    Schedule Value;       !- Actuated Component Control Type
```

In this configuration, *IRPowerFrac* is the control schedule referenced in the IR heater object (see Figure 3.9). Through this actuator, the EMS program writes the required power fraction to the schedule, thereby modulating the IR panel output during the simulation.

EMS control logic

The EMS control structure consists of several small programs that work together to evaluate zone conditions, determine occupancy mode, initialize control parameters, and compute the required infrared heating power based on the regression model.

First, a dedicated EMS program computes the average internal surface temperature of the zone to get the mean wall temperature, which is required in the regression function for the main control logic. The six inside surface temperatures (four walls, floor, and ceiling) are summed and divided by six to obtain a time–varying mean value: *CalcWallTemp*. This averaging step ensures that the control algorithm responds to the overall thermal state of the enclosure rather than to a single surface.

A second program, *ManageOccupancyMode*, governs the basic operating mode of the system. When the sensor detects at least one occupant in the room, the infrared heater is activated to provide rapid comfort. While in the absence of occupants, the IR heater is switched off. The gas boiler remains always available to maintain baseline temperature, which can be influenced by changing the heating setpoint in this program. This keeps the logic simple and prevents unnecessary operation during unoccupied periods.

The experimental work provides an empirical relationship between the PMV, mean air temperature T_{air}, mean wall temperature T_{wall}, surface emissivity ε, and IR heater power P_{IR}. The original regression form obtained from chamber measurements is given by:

$$\begin{aligned} \text{PMV} = &-0.1703 \\ &+0.02624\,(T_{\text{wall}} - 16.5) \\ &+0.1643\,(T_{\text{air}} - 19) \\ &-0.1572\,(\varepsilon - 0.5) \\ &+0.0002108\,(P_{\text{IR}} - 360) \\ &+0.4069\,(\varepsilon - 0.5)(\varepsilon - 0.5) \\ &-0.000245\,(\varepsilon - 0.5)(P_{\text{IR}} - 360) \end{aligned} \tag{3.1}$$

The following steps reformulate the regression model into an expression that directly returns the infrared heater power P_{IR} as a function of the remaining variables. This rearranged form is required so that P_{IR} can be used within the EMS control algorithm to modulate the heater output. Original expression consists of two components:

$$\text{PMV} = \text{Base PMV} + \big(0.0002108 - 0.000245(\varepsilon - 0.5)\big)\,(P_{\text{IR}} - 360) \tag{3.2}$$

(i) a base PMV independent of IR heater power
(ii) a sensitivity term that describes how PMV changes with P_{IR}

The coefficient that depends on IR heater power can be grouped and defined as CPIR. Thus, for the chamber:

$$\mathrm{CPIR}_{\mathrm{chamber}} = 0.0002108 - 0.000245(\varepsilon - 0.5) \tag{3.3}$$

which represents the slope of PMV with respect to IR heater power as observed in the controlled climate chamber experiment. Because the regression was derived in a small test chamber, the sensitivity must be scaled to match the larger area of the building model. The scaling factor is defined as:

$$f = \frac{A_{\mathrm{room}}}{A_{\mathrm{chamber}}} \tag{3.4}$$

where
f: Scaling factor,
A_{room}: Total surface area of the simulation zone,
A_{chamber}: Total surface area of the experimental chamber.

Here, the scaling was based on the total surface area of the respective zones. Further, applying this scaling factor to $\mathrm{CPIR}_{\mathrm{chamber}}$:

$$\mathrm{CPIR}_{\mathrm{scaled}} = \frac{\mathrm{CPIR}_{\mathrm{chamber}}}{f} \tag{3.5}$$

This ensures that the EMS correctly accounts for the fact that, in a larger room, a given IR power output produces a smaller change in perceived thermal comfort than in the small test chamber.

In EMS, the target comfort condition is defined by selecting a desired PMV setpoint $\mathrm{PMV}_{\mathrm{target}}$, arranging the equation 3.2 gives:

$$\mathrm{PMV}_{\mathrm{target}} = \text{Base PMV} + \mathrm{CPIR}_{\mathrm{scaled}}\,(P_{\mathrm{IR}} - 360) \tag{3.6}$$

Rearranging the regression function to solve for the required IR heater power yields:

$$P_{\mathrm{IR}} = 360 + \frac{\mathrm{PMV}_{\mathrm{target}} - \text{Base PMV}}{\mathrm{CPIR}_{\mathrm{scaled}}} \tag{3.7}$$

Equation (3.7) forms the foundation of the EMS control algorithm. This main control logic is implemented in the program called *ControlIR_FromRegression*. At each timestep, the EMS reads the current mean air temperature, wall temperature, emissivity, evaluates the base PMV, and then determines the required panel power needed to reach the target PMV with the help of the derived relation (3.7). The computed power is then normalized by the maximum IR power to obtain a dimensionless fraction between 0 and 1. This fractional value is passed to the *IRPowerFrac* actuator, which ultimately drives the infrared panel. The result is a dynamically modulated IR heater that activates only when occupants are present and adjusts its output to avoid both overheating and underheating while minimizing delivered heating energy.

Finally, all EMS programs are assigned to appropriate calling points. For example, the occupancy and regression controller are evaluated before the zone heat balance is initialized at each

timestep. This ensures that the updated IR power is consistently applied within the correct sequence of the EnergyPlus simulation.

3.5 Overview of simulation cases

To evaluate the proposed heating strategy in a consistent and systematic way, the simulations in this study were organized around eight IDFs. These IDFs represent the four fundamental combinations of building type and envelope quality that form the basis of the analysis:

- Simple house — old envelope
- Simple house — new envelope
- Hotel guestroom — old envelope
- Hotel guestroom — new envelope

Since each building envelope combination must be tested with both heating approaches (conventional gas heating and the new IR heating). This results in a total of eight base IDF files.

Additional parameters, namely occupancy pattern (living room vs. dining room) and climate type (Minneapolis vs. Stuttgart), are applied within these eight base files. This ensures that every comparison is made on an identical building representation, and only the desired parameter changes between simulations. Thus,

$$\begin{aligned} &4\,\text{building–envelope configurations} \times 2\,\text{heating systems} \\ &\quad \times 2\,\text{weather types} \times 2\,\text{occupancy patterns} = 32\,\text{cases}. \end{aligned}$$

Overall, this results in a total of 32 simulation cases derived from the eight base IDFs. All simulation combinations are summarized in Table 3.6.

No.	Building model	Heating system	Envelope	Climate	Occupancy
1	Simple house	Gas heating	Old	Minneapolis	Living room
2	Simple house	New IR heating	Old	Minneapolis	Living room
3	Simple house	Gas heating	New	Minneapolis	Living room
4	Simple house	New IR heating	New	Minneapolis	Living room
5	Simple house	Gas heating	Old	Stuttgart	Living room
6	Simple house	New IR heating	Old	Stuttgart	Living room
7	Simple house	Gas heating	New	Stuttgart	Living room
8	Simple house	New IR heating	New	Stuttgart	Living room
9	Simple house	Gas heating	Old	Minneapolis	Dining room
10	Simple house	New IR heating	Old	Minneapolis	Dining room
11	Simple house	Gas heating	New	Minneapolis	Dining room
12	Simple house	New IR heating	New	Minneapolis	Dining room
13	Simple house	Gas heating	Old	Stuttgart	Dining room
14	Simple house	New IR heating	Old	Stuttgart	Dining room
15	Simple house	Gas heating	New	Stuttgart	Dining room
16	Simple house	New IR heating	New	Stuttgart	Dining room
17	Hotel guestroom	Gas heating	Old	Minneapolis	Living room
18	Hotel guestroom	New IR heating	Old	Minneapolis	Living room
19	Hotel guestroom	Gas heating	New	Minneapolis	Living room
20	Hotel guestroom	New IR heating	New	Minneapolis	Living room
21	Hotel guestroom	Gas heating	Old	Stuttgart	Living room
22	Hotel guestroom	New IR heating	Old	Stuttgart	Living room
23	Hotel guestroom	Gas heating	New	Stuttgart	Living room
24	Hotel guestroom	New IR heating	New	Stuttgart	Living room
25	Hotel guestroom	Gas heating	Old	Minneapolis	Dining room
26	Hotel guestroom	New IR heating	Old	Minneapolis	Dining room
27	Hotel guestroom	Gas heating	New	Minneapolis	Dining room
28	Hotel guestroom	New IR heating	New	Minneapolis	Dining room
29	Hotel guestroom	Gas heating	Old	Stuttgart	Dining room
30	Hotel guestroom	New IR heating	Old	Stuttgart	Dining room
31	Hotel guestroom	Gas heating	New	Stuttgart	Dining room
32	Hotel guestroom	New IR heating	New	Stuttgart	Dining room

Table 3.6: Overview of all simulation scenarios considered in the analysis

4. Results and Discussion

This chapter presents the simulation results for all 32 cases in a structured and systematic way. It begins with an analysis of the operational behavior of both heating systems, followed by the zone thermal energy balance. The chapter then compares the heating systems in terms of energy end use, greenhouse gas emissions, and operational fuel costs. Finally, the key findings are summarized and discussed.

To produce simulation results in EnergyPlus, the model timestep needs to be defined. In this study, the timestep was assessed by comparing simulations with a 10-minute and an hourly timestep. The generated daily profiles, as well as the total energy use, showed no meaningful differences between the two settings. Therefore, the hourly timestep was selected for all simulations, as it provides sufficient temporal detail while reducing computational effort. As a result, the occupancy patterns change only at full hours and not within the hour.

In addition, it is important to note that all results reported in this section are specific to the heating period. Since the primary objective of this study is to evaluate heating system performance and identify potential energy savings, the summer period, during which the heating system remains inactive, is not considered. Consequently, no results are shown for these times.

4.1 Operational patterns

Before comparing the energy end use of the different heating systems, it is essential to first understand how each system operates in the simulation. This section, therefore, illustrates the daily and seasonal behavior of both the reference gas heating system and the proposed IR heating approach. The aim is to verify that each system performs according to the intended control strategy and to show how their operation differs in practice.

In addition to the daily profiles, an example of the annual space heating demand is also presented. This highlights the seasonal on/off behavior of the heating systems and provides context for the later comparison of energy use and emissions.

Reference case

This section presents the simulation results of the base case using traditional gas heating. The objective is to illustrate how the gas heating system operates and meets the heating demand throughout the heating season. This serves as a reference for the assessment of the proposed IR heating strategy. In this results section, the proposed IR heating system is mainly compared with conventional gas heating. Therefore, the terms reference case, base case, and conventional heating are used alternatively throughout this section to refer to the gas heating system, i.e., the gas boiler.

To understand the annual heating behavior, the space heating profile of the simple house model under Minneapolis weather conditions is shown in Figure 4.1. The profile reflects the typical seasonal pattern, with significantly higher heating demand during the winter months. As discussed in the previous chapter, the heating system is turned off during summer (on/off dates were determined using a moving average approach) to match the realistic seasonal operations. Therefore, no heating appears in the profile during that period.

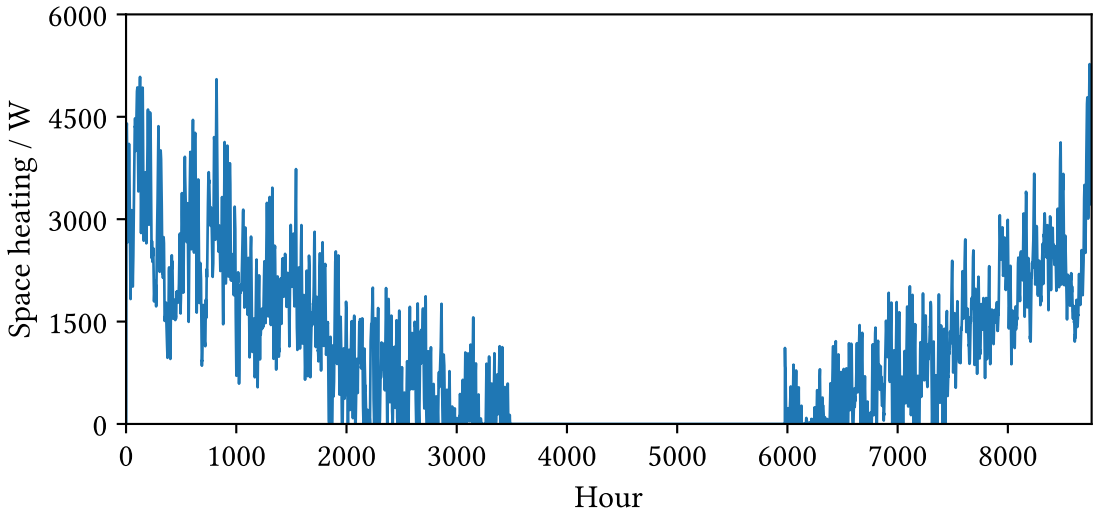

Figure 4.1: Reference space heating end use profile in Minneapolis weather conditions starting from January

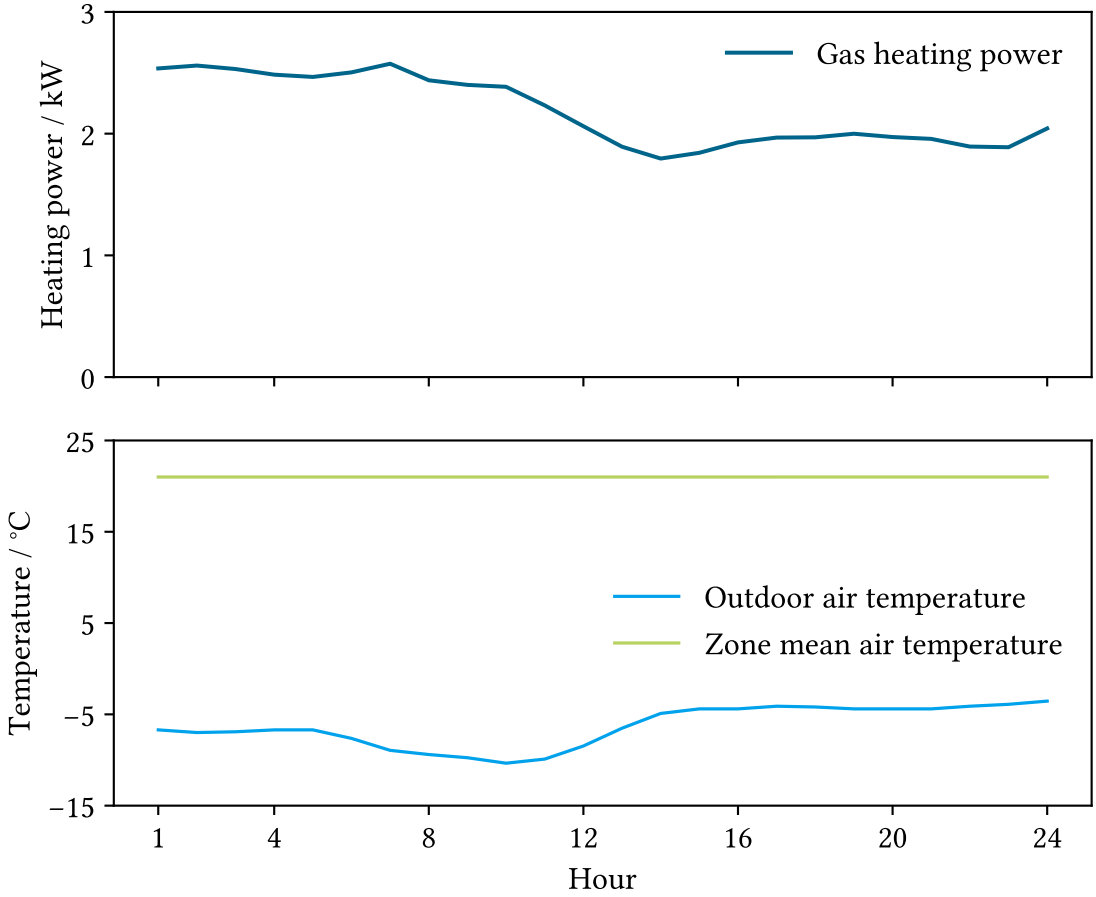

Figure 4.2: Daily running pattern of gas heating with respect to outdoor air temperature in order to maintain the desired zone air temperature

To better illustrate the operational behavior of the gas heating system, Figure 4.2 shows the daily heating pattern for a typical winter day (11 January). The plot also includes both the zone mean air temperature and the outdoor air temperature. As discussed in the simulation chapter, the gas heater is modeled as an ideal heater with autosizing feature, meaning it is always capable of supplying sufficient heat to maintain the indoor setpoint temperature. For the base case, this setpoint was set to 21 °C.

The figure confirms this behavior, as can be seen that under varying outdoor conditions, the indoor air temperature remains consistent with the setpoint throughout the day.

New IR heating

In this section, the performance of the proposed IR heating system is presented based on the simulation results. The operating pattern of the system is illustrated in Figure 4.3, which shows the daily heating behavior for a typical winter day (11 January). As shown, the gas boiler and the IR heating panel operate in a coordinated manner so that the boiler provides the base heating, while the IR panel activates only when an occupant is present in the zone.

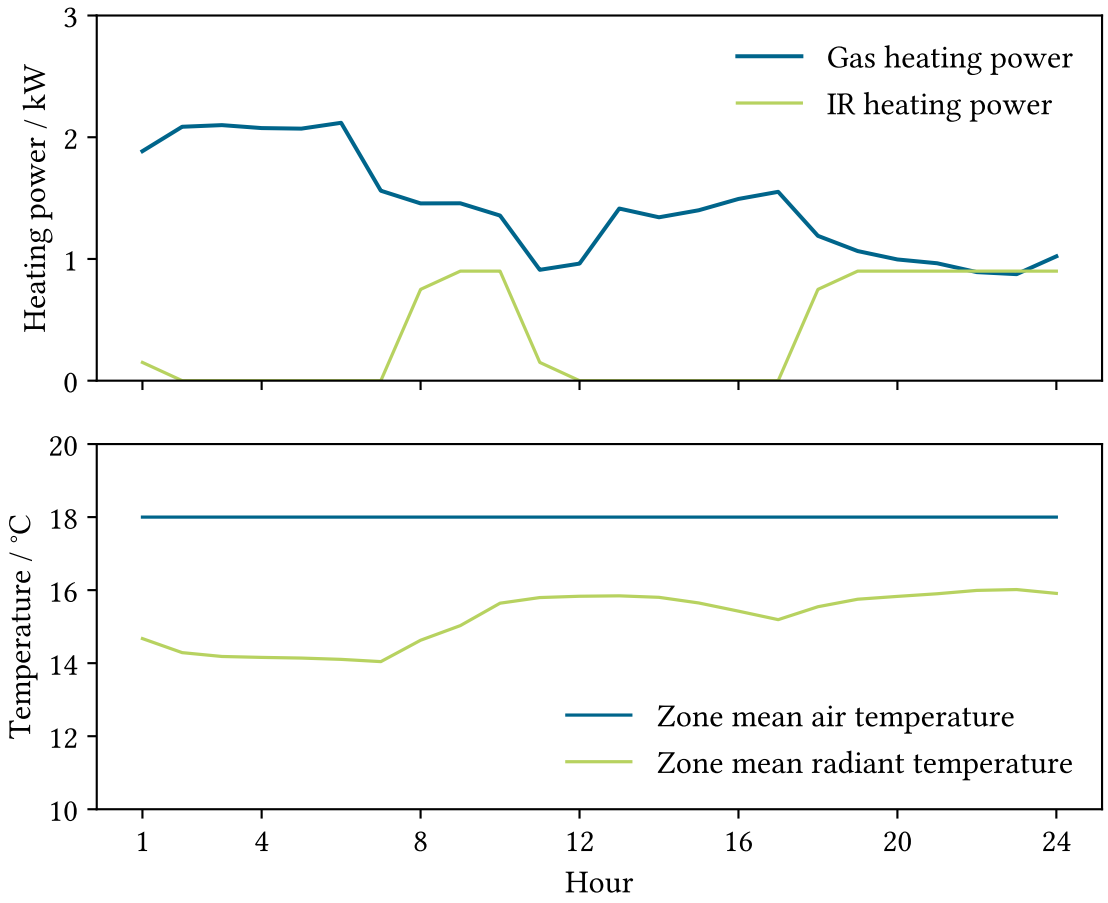

Figure 4.3: Daily running pattern of IR and gas heating strategy

The figure also includes both the zone mean air temperature and the mean radiant temperature. The gas boiler is mainly responsible for keeping the air temperature at the reduced

setpoint of 18 °C, as clearly visible in the plot. In contrast, the IR heater primarily influences the mean radiant temperature. Each time the IR panel activates, a clear rise in the radiant temperature can be observed, demonstrating its targeted contribution to improving perceived thermal comfort without raising the air temperature.

The influence of this new IR heating strategy on thermal comfort can be observed in Figure 4.4, which presents the PMV profile for the same winter day shown previously in Figure 4.3. In the figure, the black dashed line represents the neutral or optimum comfort level (PMV = 0), while the blue curve indicates the actual PMV inside the zone throughout the day. The shaded gray regions correspond to the periods during which the occupants are present.

A clear pattern can be observed, whenever the occupant enters the space (around 08:00, and again between 17:00 and 23:00), the IR heater activates. Correspondingly, the PMV value rises rapidly toward the neutral comfort level. This quick improvement in perceived comfort is exactly the desired outcome of the proposed strategy. The results indicate that the IR system effectively boosts thermal comfort during occupied periods, achieving the goal of providing faster and on demand comfort compared to conventional heating alone.

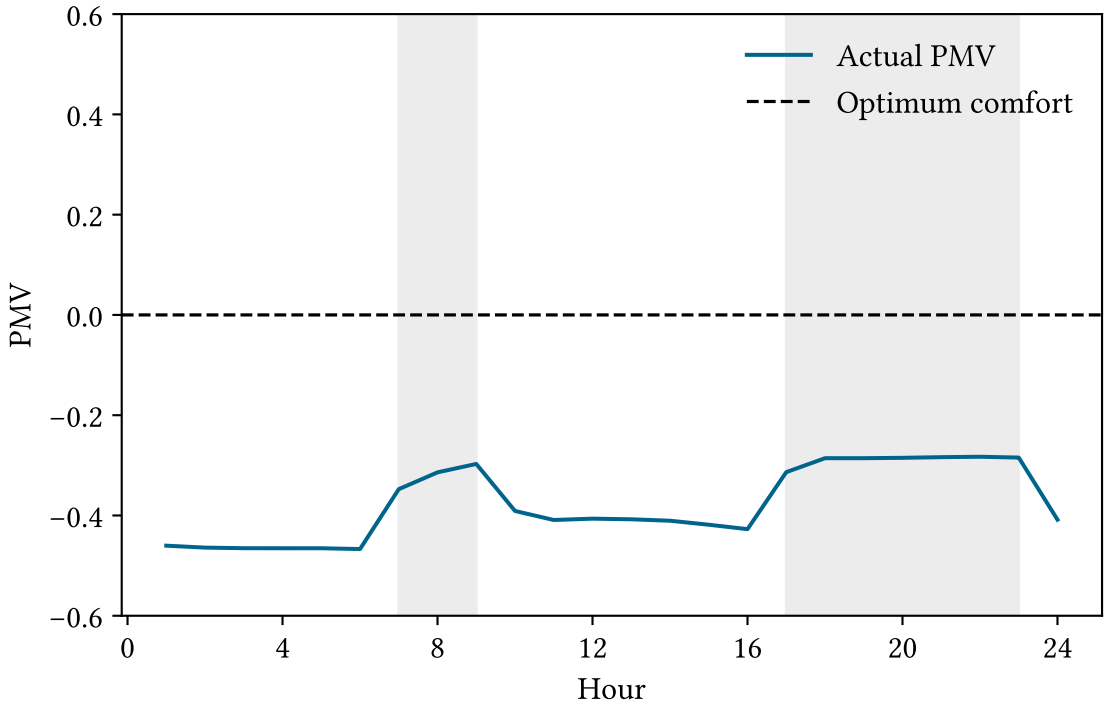

Figure 4.4: PMV of an occupant throughout the day compared to the optimum comfort line, gray shading shows occupant presence

To ensure acceptable thermal comfort, the average PMV during occupied hours over the heating period was evaluated and verified to remain within the acceptable limits given by the ASHRAE standard, as discussed in Chapter 2. For this reason, the air temperature setpoint was fixed at 18 °C. Lower setpoints were initially tested, but they resulted in average PMV values outside the acceptable comfort range. However, detailed PMV results are not presented here, as thermal comfort was not the focus of this study.

4.2 Thermal energy balance of the zones

It is essential to understand the thermal energy balance of the zones before comparing the different heating systems. For both reference building models used in this study, the single zone house and the hotel guestroom, the main components of the energy balance are considered. This analysis confirms that the house model has a high heating demand, whereas the hotel guestroom represents a low heating demand zone.

The results illustrate how the required space heating compares to all the available internal heat gains, and therefore how much these internal gains contribute to covering the heating demand. Moreover, it gives the heat losses through the building envelope and quantifies their relative contribution to the overall heat load of the zone. Understanding these interactions offers a good foundation for interpreting the later comparison between the traditional gas heating system and the proposed infrared heating setup.

Moreover, all presented heat losses and gains are evaluated only for the heating period. To ensure consistency between both models, the Minneapolis climate and the old envelope combination is used to analyze and compare the thermal energy balance of the zones.

Simple house model

The overall thermal energy balance of the simple house model is summarized in this section. As shown in the Figure 4.5, all three heat loss mechanisms contribute significantly to the total heat losses of the model.

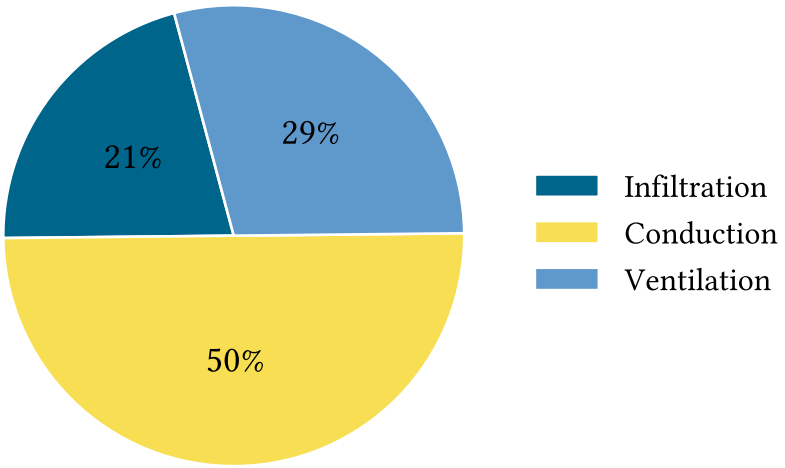

Figure 4.5: Heat losses from the zone (under Minneapolis weather and old envelope)

Conduction accounts for 50% of the total losses. This is expected, as the zone is defined by four outer walls directly exposed to the outdoor environment, resulting in larger conductive heat transfer to the surroundings. Infiltration and ventilation also contribute notably. For this thermal energy balance, the Minneapolis climate and the old building envelope are considered, representing cold outdoor conditions and a leaky envelope, which together result in high heat losses through all major loss paths. In total, it leads to around 10111 kWh of heat loss during

the heating period. These values reflect the continuous air exchange with the outdoor air, which gradually increases the heat load on the heating system.

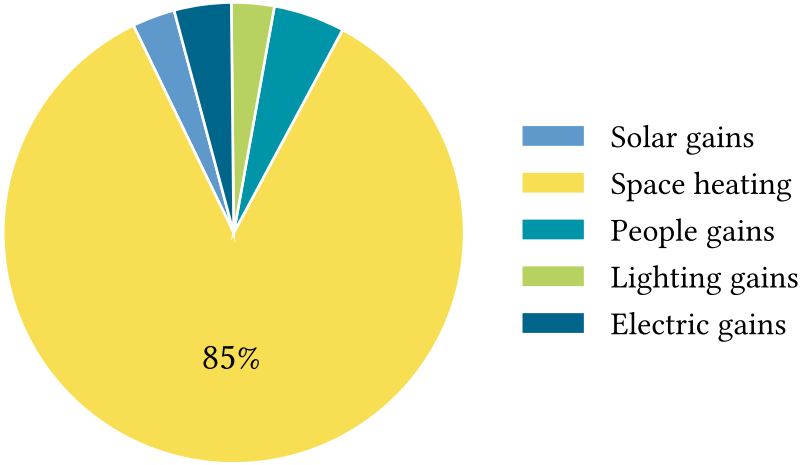

Figure 4.6: Heat gains inside the zone (under Minneapolis weather and old envelope)

After examining the heat losses, Figure 4.6 presents the distribution of heat gains within the simple house model. It is evident that space heating dominates the total gains, contributing approximately 85%, while all other internal gains, such as solar, occupants, lighting, and electrical equipment or plug loads, collectively account for only 15%. This indicates that internal gains play only a minor role in supporting the heat demand of the zone, which in turn explains the high dependency on space heating.

Due to the detached nature of the building model, which results in higher heat losses and very low internal heat gains, the simple house model shows a high space heating demand. The heating energy end use results are discussed in the following sections.

Hotel guestroom

A similar thermal energy balance analysis is done for the hotel guestroom as well. Figure 4.7 shows that space heating accounts for approximately 48% of the total heat gains in the zone, while the remaining demand is covered by the internal gains. Among these, electrical equipment contributes the highest around 22%, and the gains from lighting and occupants are also apparent. Compared to the simple house model, the hotel guestroom shows a significantly lower relative demand for space heating. That can be justified by examining the corresponding heat loss distribution.

As discussed earlier, the hotel guestroom is surrounded by adjacent heated zones, and only one wall is directly in contact with the outdoor environment. This geometry naturally lowers the transmission or conduction heat losses to the ambient air, which can be noticed in the Figure 4.8. The simulation results confirm this, as the total heat loss during the heating period for the guestroom is approximately 3683 kWh, which is significantly lower than the 10111 kWh observed in the simple house model.

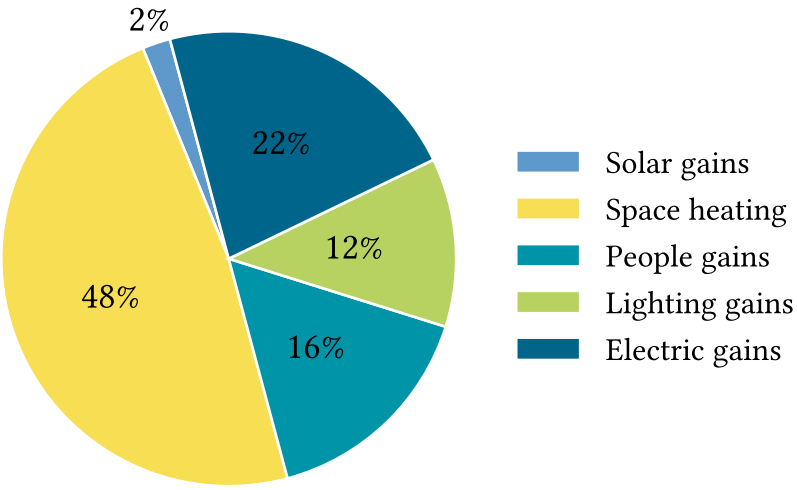

Figure 4.7: Heat gains inside the hotel guestroom (under Minneapolis weather and old envelope)

This reduction is primarily due to the much smaller conductive heat loss area. However, the values also show that infiltration becomes the dominant loss mechanism in the guestroom, because the results are for the model with an older, leakier building envelope, allowing more cold outdoor air to enter the zone. Overall, the guestroom benefits from its position within a multi story building, which leads to substantially lower overall heat losses compared to the standalone single zone house.

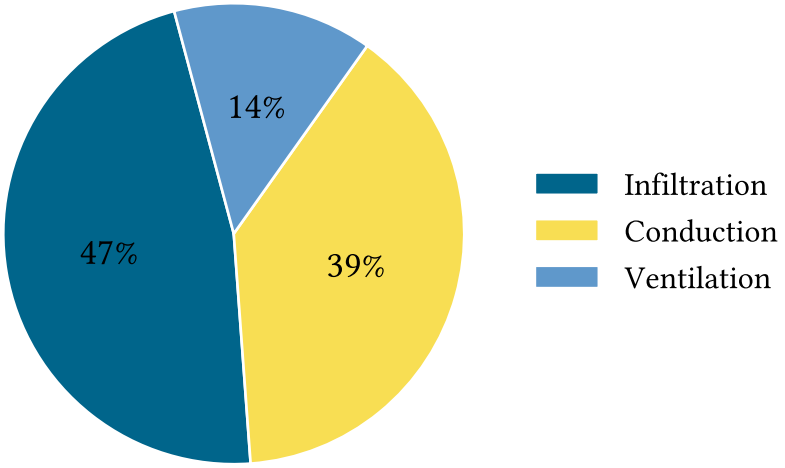

Figure 4.8: Heat losses from the hotel guestroom (under Minneapolis weather and old envelope)

4.3 Energy end use

In this section, the energy end use inside the zone is compared across all scenarios for both building models with the goal of quantifying the energy savings. To keep the results clear,

each comparison graph includes the outcomes from eight simulations. These are arranged in four pairs, where each pair represents one specific scenario.

The four scenario pairs displayed in each graph are:

- **Old_Mnp** — Old envelope in Minneapolis weather conditions
- **New_Mnp** — New envelope in Minneapolis weather conditions
- **Old_Stuttgart** — Old envelope in Stuttgart weather conditions
- **New_Stuttgart** — New envelope in Stuttgart weather conditions

These four pairs allow a structured comparison based on two key aspects. First, the climatic conditions (cold climate vs. moderate climate) and second, the building age (old vs. new envelope). For other variables like occupancy patterns, separate graphs are prepared following the same grouping logic. Moreover, each pair contains two bars:

- the first bar represents the reference case with conventional gas heating,
- the second bar represents the new IR heating approach.

That means, the **energy savings** for each scenario can be directly interpreted as the difference between the two bars in a given pair. This section provides only a graphical overview of the results. Detailed and exact numerical values for both building models and all scenarios are summarized in Appendix A-2.

Simple house model

Building upon the previous discussion of the graph patterns, this section provides the results for the simple house model. The outcomes based on the two chosen occupancy patterns are shown.

Living room occupancy

Figure 4.9 shows the energy end use for the eight simulated cases based on weather conditions and building envelope quality. The results correspond to the living room occupancy pattern, which represents a longer duration of occupant presence. Across all scenarios, the base use remains identical. This reflects non-heating electricity use, mainly lighting and plug loads and is kept constant to ensure a fair comparison between the different heating strategies.

A similar pattern can be observed across all four pairs in Figure 4.9. For the new heating approach, the total energy end use is significantly reduced in all cases when compared to the baseline case. These exact reductions are highlighted by the downward facing green arrows shown for each pair.

Among all cases, the combination of an old envelope and the Minneapolis climate shows the largest energy savings, reaching 2892 kWh per year (33% reduction compared to the reference case). In contrast, the new envelope with Stuttgart weather shows the smallest absolute reduction of about 1387 kWh. However, this still corresponds to a higher relative reduction of 35%, indicating greater efficiency in building with a better envelope and milder climate.

With a better envelope quality and moderate weather, the reference case already requires substantially less heating energy, leaving less potential for savings when switching to the proposed new heating. As a result, the absolute energy savings decrease when moving from the

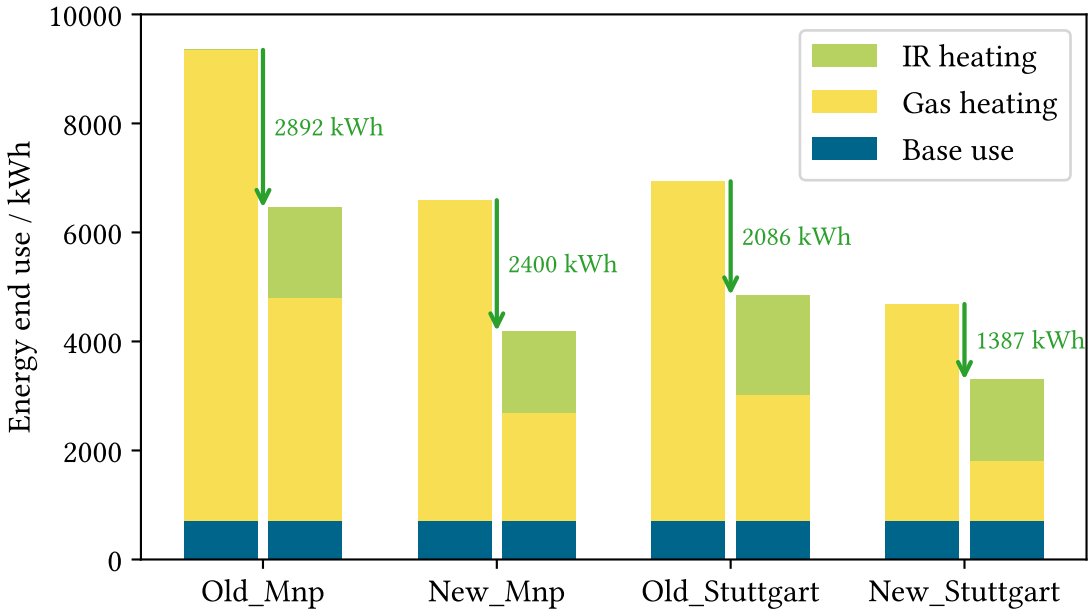

Figure 4.9: Energy end use reductions with IR heating compared to respective base cases with living room occupancy pattern

old to the new envelope and from the Minneapolis to the Stuttgart climate. These results are based on the living room occupancy profile and the following plot refers to the outcomes for the dining room occupancy.

Dining room occupancy

Figure 4.10 presents the results for the dining room occupancy pattern in the simple house model. This pattern represents short-duration occupant presence. Therefore, the demand for thermal comfort and the activation of the IR heater are lower than in the living room occupancy pattern.

A similar behavior to the living room case can be observed. All four scenarios show a decreasing trend in energy use when the new heating approach is applied. The highest energy savings occur in the case with the old envelope and Minneapolis weather site, reaching 3258 kWh, which corresponds to a 37% reduction compared to the reference base case. Like the living room results, the new envelope shows lower absolute savings but higher efficiency in relative terms. In particular, the new envelope in the Minneapolis climate achieves the highest relative reduction of 47%. Overall, across all four scenarios, higher energy savings can be observed than in the living room occupancy pattern.

Because the dining room is occupied less frequently, the IR heater operates for fewer hours, while the gas heating maintains the base setpoint temperature throughout the day. As a result, the dining room occupancy pattern produces comparatively higher energy savings across all four scenarios.

Figure 4.11 presents the relative reductions in heating energy end use for all four scenarios compared to their respective reference cases. It compares the results of the living room and the dining room occupancy patterns.

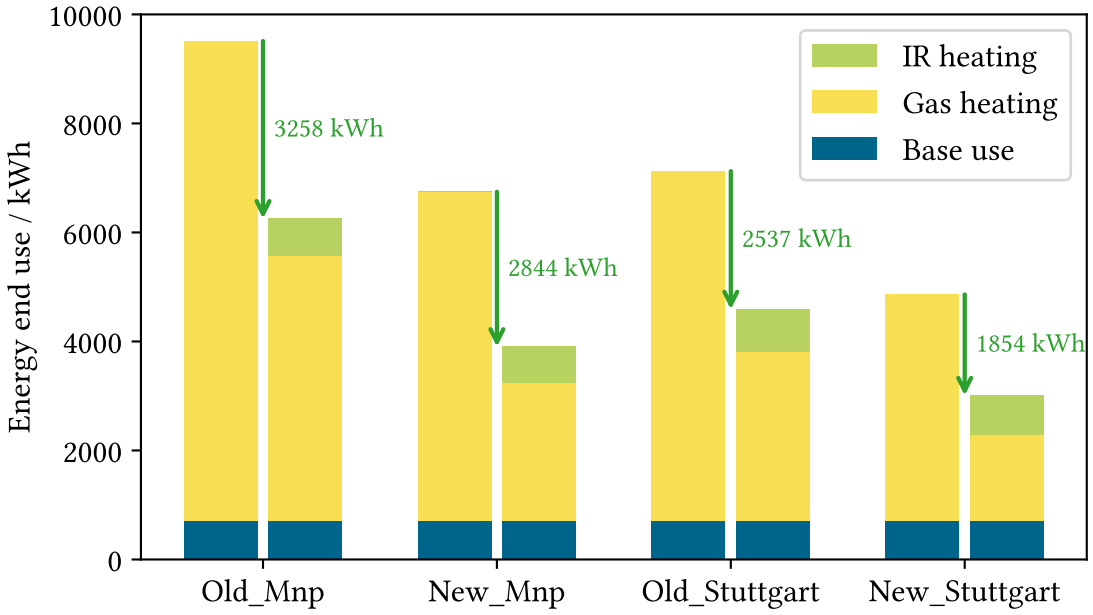

Figure 4.10: Energy end use reductions with IR heating compared to respective base cases with dining room occupancy pattern

The dining room occupancy pattern achieves higher relative savings compared to the living room across all scenarios, with a maximum reduction of 47%. In addition, buildings with a new or improved envelope show smaller absolute savings but perform relatively better, resulting in higher relative reductions.

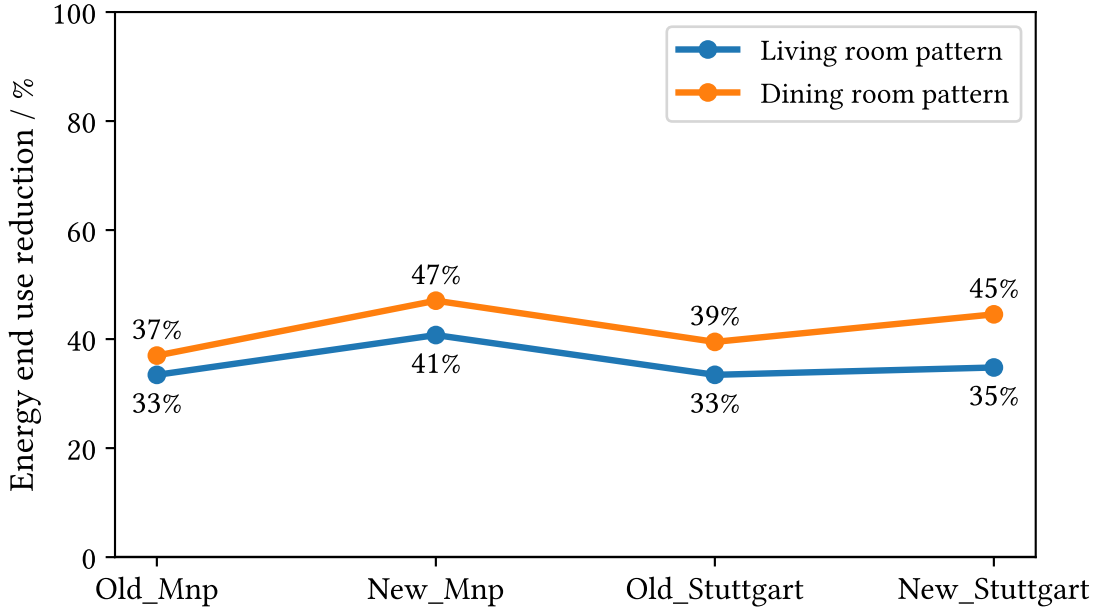

Figure 4.11: Comparison of relative heating energy end use reductions compared to their respective base case for living room and dining room occupancy

Thus, buildings with old envelopes show larger energy reductions and climate impact, while better-insulated buildings achieve smaller climate benefits.

Hotel guestroom

This section provides the results from the hotel guestroom model. Similar to the simple house results, the energy end use and the respective reduction based on the two chosen occupancy patterns are shown below for each scenario.

Living room occupancy

Figure 4.12 presents the results for the living room occupancy pattern in the hotel guestroom. As shown, the new IR heating approach leads to a reduction in total energy end use across all four scenarios. The base energy use remains almost identical to that of the simple house model, as it mainly reflects lighting and plug loads. However, the overall energy demand of the guestroom is noticeably lower. This aligns with the thermal energy balance discussed earlier, since the guestroom is surrounded by adjacent conditioned rooms, the need for space heating is significantly reduced.

As a result, the absolute energy savings achieved with the IR heating strategy are smaller compared to the single house model. Among the four scenarios, the old envelope with Stuttgart weather shows the greatest reduction, achieving a yearly saving of approximately 543 kWh.

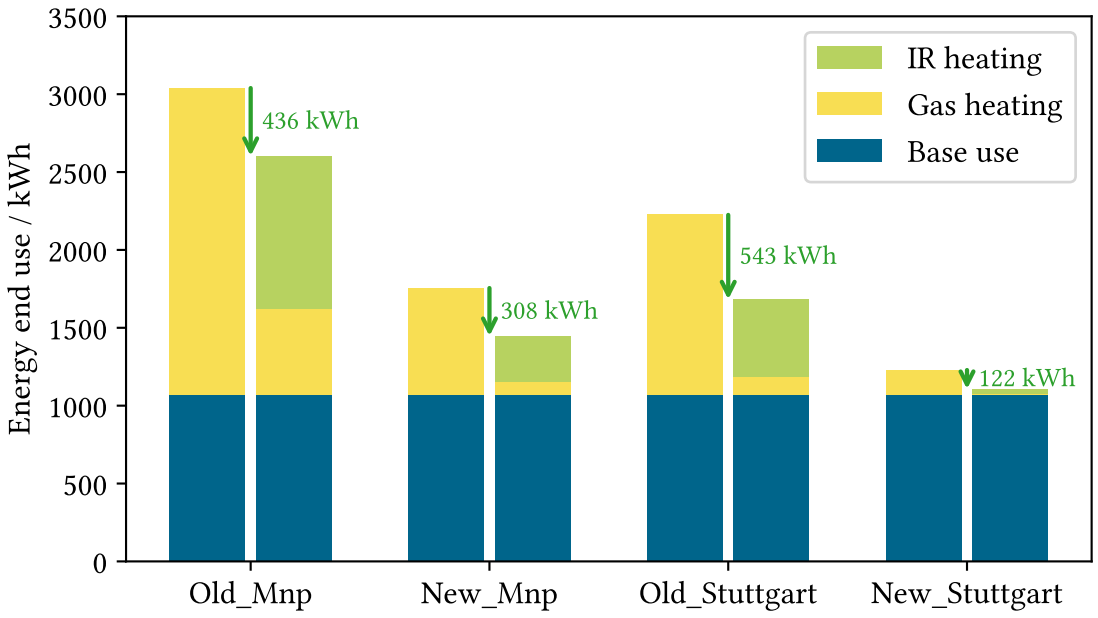

Figure 4.12: Energy end use reductions with IR heating compared to respective base cases with living room occupancy pattern

Here as well, the comparative savings are smaller for the better (new) envelope quality. This is expected, since the old envelope is more porous and allows higher infiltration of cold air from outside, which increases the heating demand. Because of this higher baseline consumption, the potential for energy savings is larger in the old envelope cases compared to the better insulated scenarios.

Dining room occupancy

Figure 4.13 presents the results for the dining room occupancy profile in the hotel guestroom model. As in the living room case, all four scenarios show a reduction in total energy end use when applying the new heating strategy.

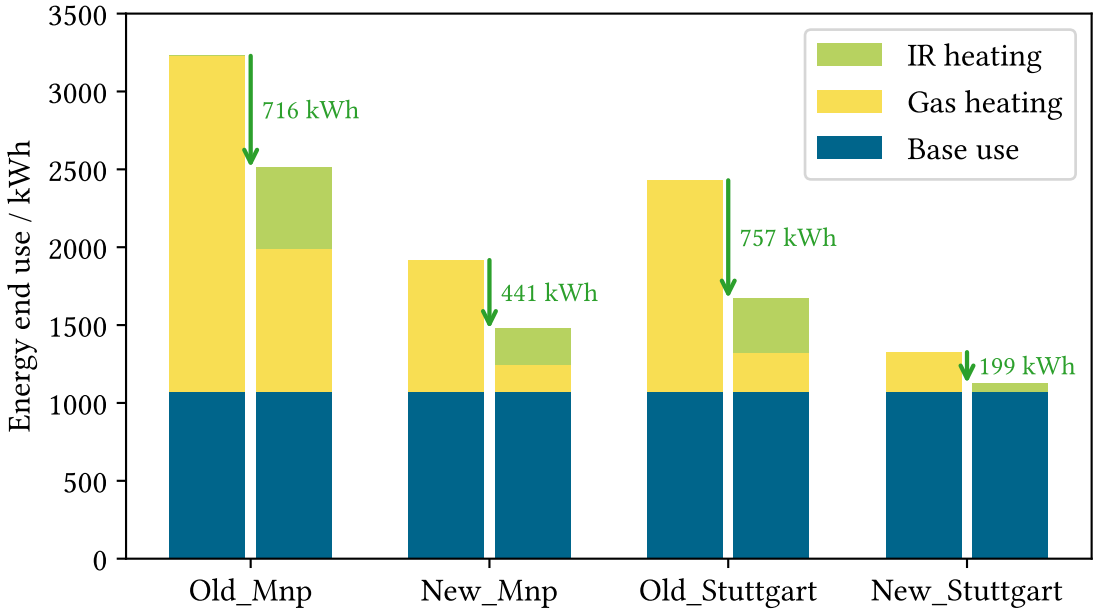

Figure 4.13: Energy end use reductions with IR heating compared to respective base cases with dining room occupancy

However, because the dining room is used less frequently, the IR heater activates fewer times compared to the living room. Moreover, unlike the reference case, the conventional system has to maintain only the base air temperature (18 °C) throughout the entire day. These two effects result in noticeably higher energy savings in all scenarios for the dining room occupancy pattern, or in general for occupancy schedules with shorter and less frequent presence. Among all cases, the old envelope under Stuttgart weather conditions shows the highest reduction, reaching 757 kWh.

Figure 4.14 shows the relative heating energy savings for the hotel model and compares the dining room and living room occupancy patterns. Similar to the house model, the dining room pattern achieves higher savings due to shorter occupancy periods.

However, in the hotel model, there is a much larger variation in savings, with relative reductions reaching up to 77% (199 kWh) for the new envelope under Stuttgart weather conditions. Unlike the house model, the hotel zone is surrounded by adjacent zones, which helps maintain indoor air temperature and significantly reduces or even eliminates the need for base gas heating in the IR strategy. As a result, gas heating is used only minimally, while the IR heater operates mainly during occupancy periods. These factors lead to higher relative reductions in the hotel model. However, in absolute terms, the total energy savings remain lower than those observed for the house model.

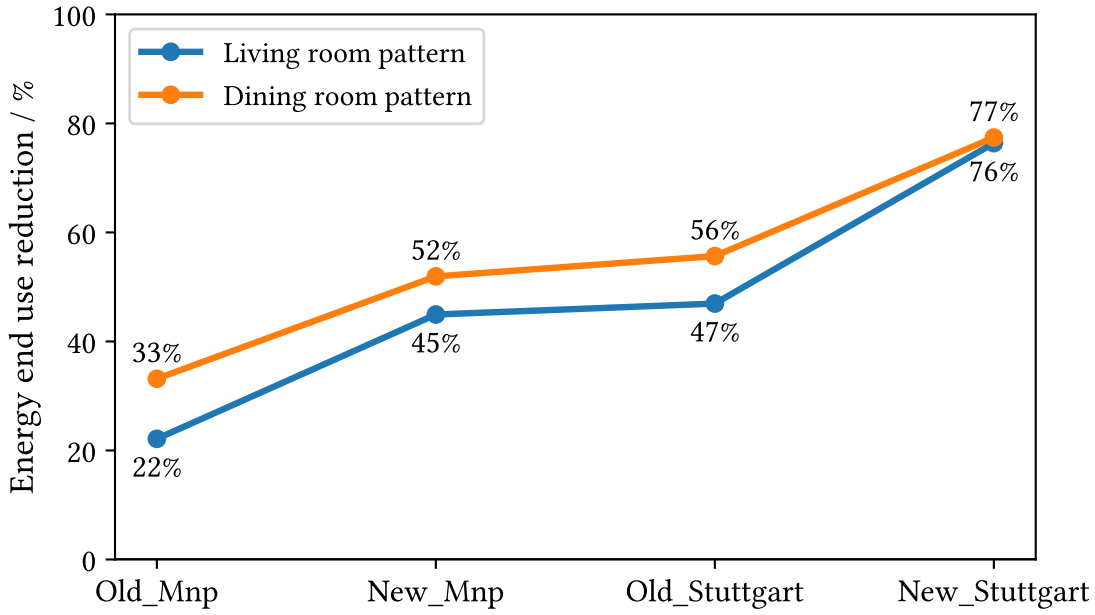

Figure 4.14: Comparison of relative heating energy end use reductions compared to their respective base case for living room and dining room occupancy

4.4 Greenhouse gas emissions

In addition to the energy comparison, the analysis also examines the associated greenhouse gas (GHG) emissions. For this purpose, CO_2-equivalent (CO_2e) emission factors are applied to the two energy carriers utilized in the heating systems, which are natural gas and grid electricity. To ensure scientific consistency, emission factors from the established standard sources are used.

The default emission factor for the stationary combustion of natural gas is provided by the *Intergovernmental Panel on Climate Change* (IPCC). According to the IPCC 2006 Guidelines, the emission factor for natural gas is 56,100 kg CO_2e / TJ [54], that converts to 0.202 kg CO_2e / kWh.

For electricity, the standard emission factor is taken from the *U.S. Environmental Protection Agency* (EPA) database [55]. The EPA states that grid-supplied electricity has an emission factor of 0.432 kg CO_2e / kWh.

The total GHG emissions for each heating setup are determined using the following general formula:

$$\text{GHG}_{\text{fuel}} = \text{Energy consumption}_{\text{fuel}} \times \text{Emission factor}_{\text{fuel}} \tag{4.1}$$

This formulation allows the direct comparison of emissions from various heating technologies based on the fuel consumed, which is determined from their respective efficiency and the final energy consumption.

Moreover, for the greenhouse gas emissions comparison, heating with the heat pump case is also included. Both the infrared heater and heat pump use electricity as a fuel, making them

directly comparable from an emissions perspective. Moreover, heat pumps are increasingly considered as a key technology for the renovation and decarbonization of residential heating systems [10]. Therefore, including a heat pump benchmark provides a meaningful reference for evaluating the proposed heating strategy.

For a simplified approach, no detailed heat pump model was implemented in EnergyPlus for this analysis. The end consumption from the conventional gas heating case was taken as the required useful heating energy. This demand was then divided by the coefficient of performance (COP) to estimate the electricity use of a heat pump providing the same heat output. A COP of 3 was selected based on typical values reported for residential heat pump systems in the literature [56], which makes an appropriate and scientifically supported assumption for this comparative emissions analysis.

Simple house model

Based on the emission factors and the methodology discussed in the previous section, Figure 4.15 presents the GHG emissions for the simple house model using the living room occupancy profile.

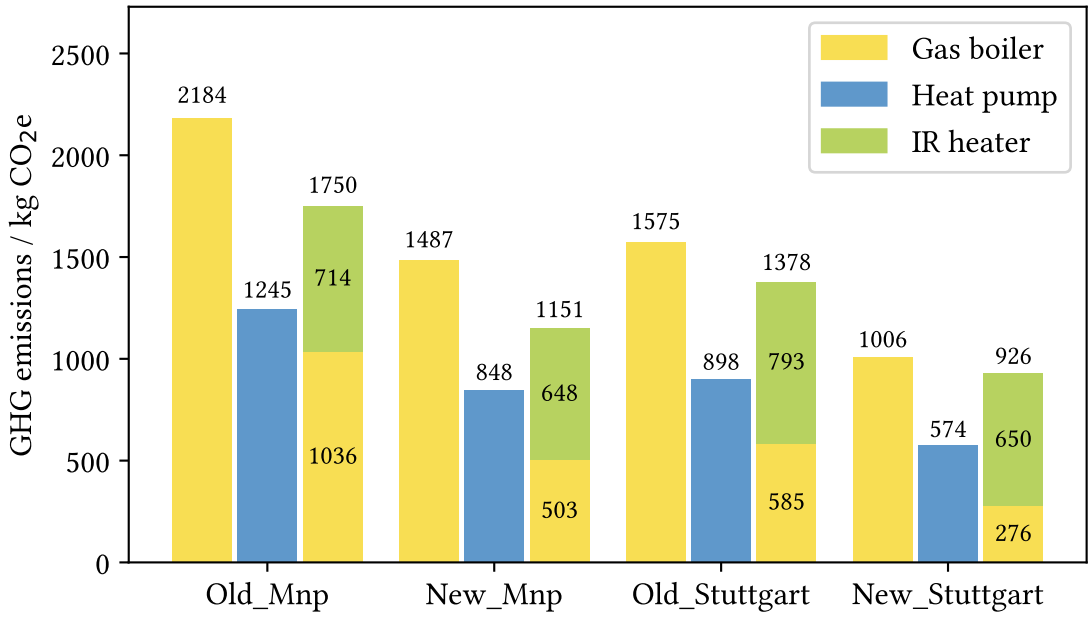

Figure 4.15: GHG emissions for the simple house model based on living room occupancy

As can be noticed, the reference case with conventional gas heating produces the highest emissions in all four scenarios. In contrast, the heat pump case results in the lowest emissions among the three heating options. Although electricity has a higher emission factor than natural gas, the heat pump's high efficiency (COP = 3) significantly reduces the required fuel input, which leads to lower overall emissions.

The proposed IR heating strategy shows emissions higher than the heat pump case, but still in all cases lower than the conventional gas boiler or the reference case. The largest absolute reduction is observed for the case with the old envelope in the Minneapolis climate conditions,

reaching savings of 433 kg CO_2e per year. This corresponds to a reduction of about 20% compared to the reference conventional heating. Overall, with this occupancy pattern, emission reductions between 8% and 20% were observed compared to the reference case.

Figure 4.16 presents the outcomes for the dining room occupancy pattern, which represents a short and less frequently used space. The reference case with conventional gas heating shows the highest emissions in all scenarios, just as observed for the living room profile. As shown, the total emissions from the proposed IR heating approach are significantly lower under the short occupancy pattern. For well-insulated cases, the emissions are even comparable to those of the heat pump system for this occupancy pattern. This is mainly because the shorter occupancy results in fewer IR heater operating hours, which reduces electricity consumption. However, the heat pump remains the lowest emission option, while conventional gas heating has the highest emissions across all four scenarios. The proposed IR heating system consistently falls between these two systems.

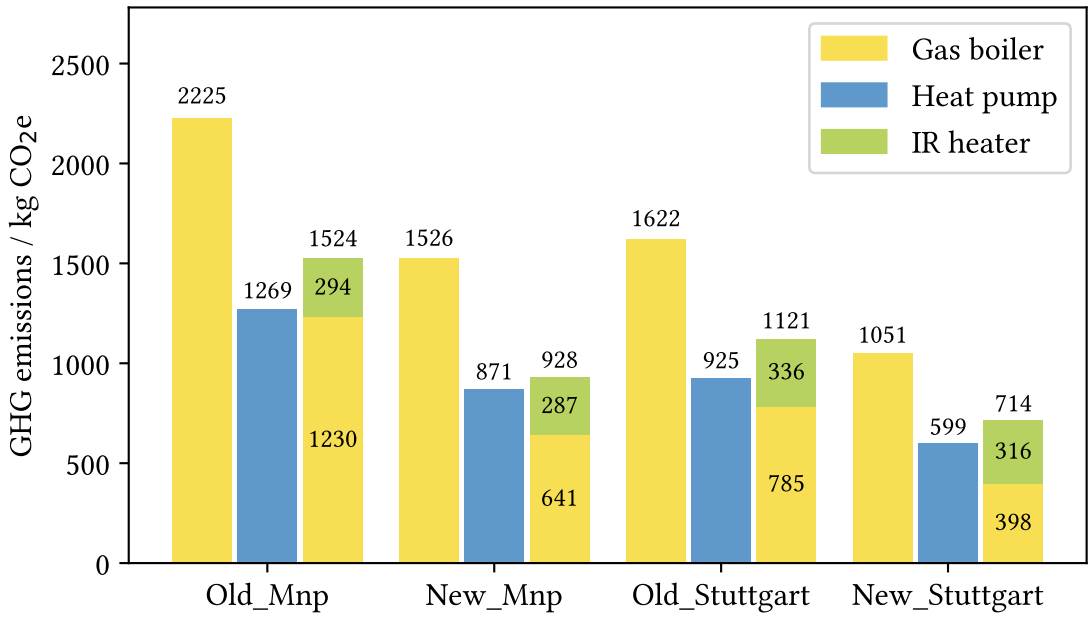

Figure 4.16: GHG emissions for the simple house model based on dining room occupancy

Once again, the greatest absolute reduction is observed for the old envelope under Minneapolis climate conditions, with annual savings of approximately 700 kg CO_2e, corresponding to a reduction of around 31% compared to the reference case. The new envelope in Minneapolis also performs well, achieving the highest relative reduction of about 39%.

Overall, across all scenarios with the dining occupancy pattern, emission reductions between 30% and 39% were observed. These results confirm that less frequent and short-duration occupancy leads to substantially higher emission reductions than longer occupancy.

Hotel guestroom

This section gives the GHG emission results for the hotel guestroom model. The first set of outcomes corresponds to the living room occupancy profile shown in the Figure 4.17.

In this case, the differences between the emissions of the proposed IR heating strategy and the reference gas system are apparently small. The only exception is the scenario with an old envelope under Minneapolis weather, where the emissions from the new IR approach are approximately 13% higher than the reference case. In all other scenarios, the IR strategy results in lower emissions than conventional gas heating, although the absolute differences are small. As expected, the heat pump generally shows the lowest emissions. However, for the case with the new envelope under Stuttgart weather conditions, the IR system produces the lowest emissions among all three heating systems, making it the most environmentally favorable option in low heating demand zones.

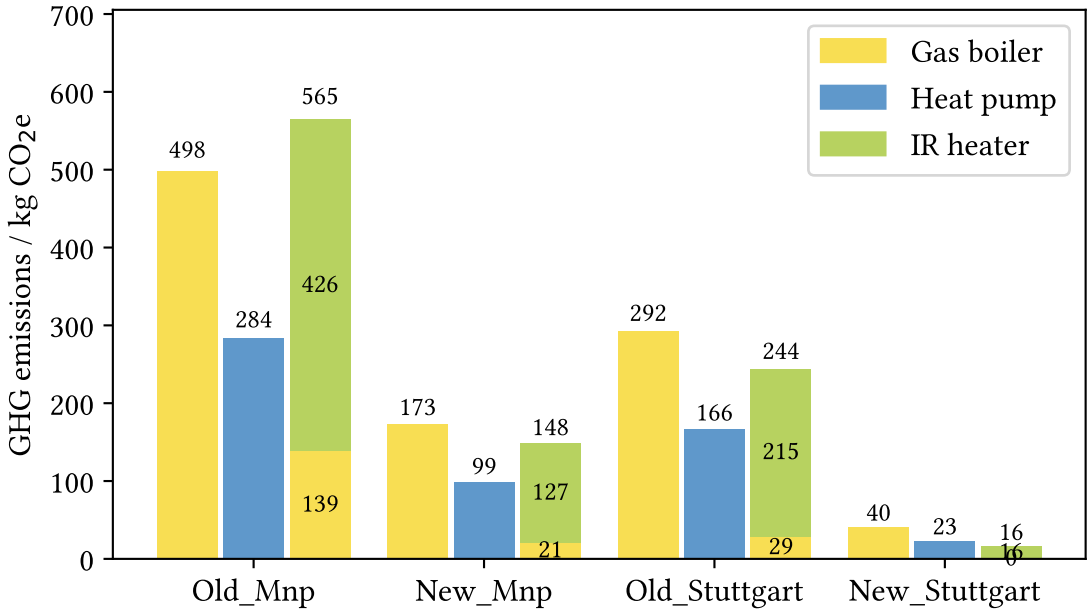

Figure 4.17: GHG emissions for the hotel guestroom model based on living room occupancy

These results can be explained by the relatively low heating demand of the hotel guestroom, as discussed in the thermal energy balance section. Because the space is partially surrounded by conditioned rooms, the baseline heating energy requirement is lower than in the simple house model. For the new heating approach, the gas boiler provides only a small fraction of the total heating, while a larger share comes from electricity used by the IR heaters because the zone is occupied frequently. Since electricity has a higher emission factor than natural gas, the overall GHG emissions of the new approach can become identical or slightly higher than the conventional systems in cases where the IR heater runs for longer periods.

After discussing the results for the living room occupancy pattern, Figure 4.18 presents the emission comparison for the dining room occupancy, which is a short-duration schedule.

Because the room is occupied for shorter periods, the IR heater is activated fewer times. As a result, the proposed IR heating strategy achieves lower emissions than the conventional gas heating system in all four scenarios. The highest emission reduction occurs for the old envelope in the Stuttgart climate, reaching savings of 128 kg CO_2e, which corresponds to a 37% decrease compared to the reference case.

The heat pump continues to be the lowest emission option in almost every scenario. The only exception is the case with the new envelope in the Stuttgart climate, where the heating demand is extremely low. In this specific situation, within the new approach, the IR heaters combined with reflective walls cover the entire small demand in an occupancy dependent way and no base gas heating is required, leading to slightly lower emissions than the heat pump and around 62% (40 kg CO_2e) reduction compared to the reference case. This illustrates how, in spaces with very low and short-duration heating needs, the IR heating approach can become particularly competitive.

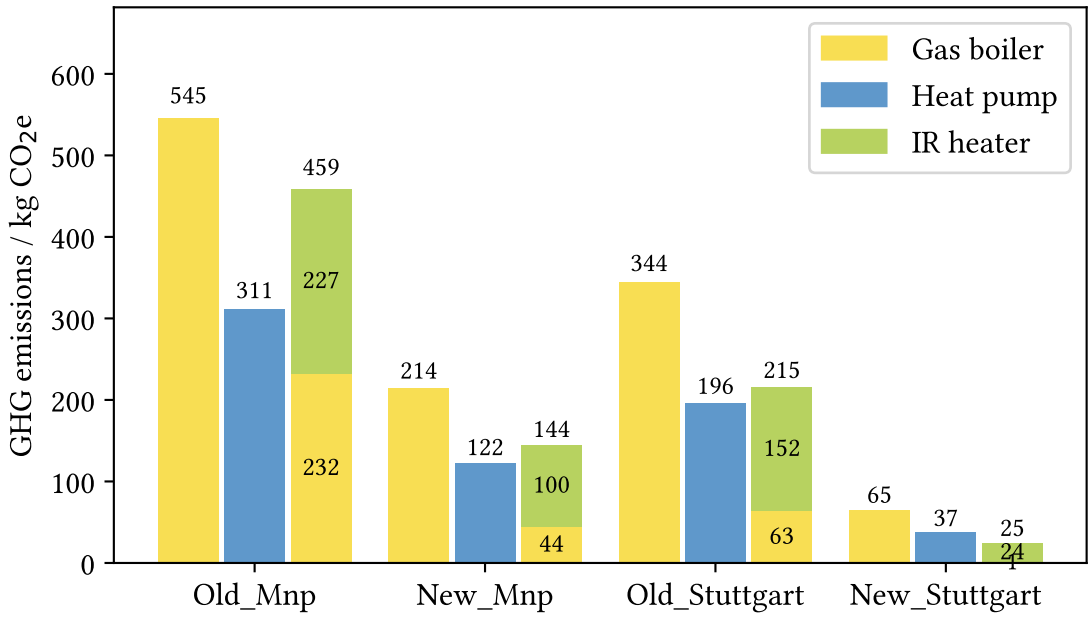

Figure 4.18: GHG emissions for the hotel guestroom model based on dining room occupancy

4.5 Operational fuel cost

This section provides an initial economic perspective by briefly comparing the operational fuel costs of the various heating systems considered in this research. A thorough cost analysis would require a more detailed assessment, including investment costs, maintenance, lifespan, and potential subsidies. The operational fuel cost comparison serves as a first step towards understanding the financial implications of the suggested heating approach. This simplified analysis allows for a quick evaluation within the scope of the current study.

For the operational fuel cost comparison, recent energy prices for German households are used. According to data from April 2025, the average electricity price is 40.1 ct/kWh, while the natural gas price is 12.3 ct/kWh [57]. These values are applied to the corresponding fuel consumption of each heating system in order to estimate their operational fuel costs. Moreover, a sensitivity analysis is performed to account for uncertainties in energy prices. Electricity prices are varied by ±25%, while natural gas prices are varied by ±50%. These ranges are chosen to represent realistic fluctuations based on the past trends and possible future developments in the energy markets.

Figure 4.19 shows the operational fuel costs for the hotel guestroom model with the living room occupancy pattern. The black lines represent the overall sensitivity results of the entire system. For the IR strategy, the white lines indicate the individual contributions from gas and electricity, while the black line shows the resulting combined sensitivity.

As shown, the proposed IR heating strategy results in higher operational costs, primarily because here significant part of its energy demand is met by electricity, which is far more expensive than natural gas. Although the heat pump relies entirely on electricity, it consistently yields the lowest operational fuel cost, reflecting its higher efficiency. The conventional gas boiler shows lower fuel costs compared to the IR heating strategy. Only in the very low heating demand case, with the new envelope and Stuttgart weather, the IR heating strategy result in the lowest fuel cost, due to the very limited operation of the IR heaters.

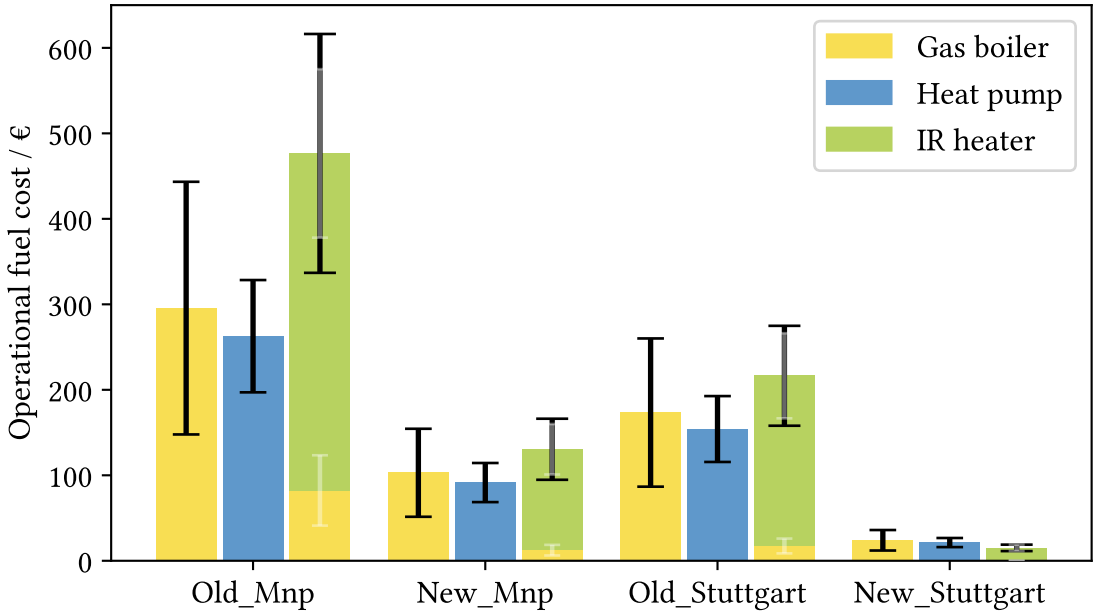

Figure 4.19: Cost hotel living

Moreover, the frequent and longer occupancy results in extended IR heater operation hours, which increases electricity use and consequently raises operational costs across all scenarios. Overall, across both models for the longer occupancy pattern, the proposed IR strategy leads to higher operational fuel costs, ranging from 2% to 60% higher compared to the reference gas heating.

The sensitivity analysis shows how operational fuel costs respond to variations in energy prices. The reference case based only on natural gas shows the largest uncertainty, particularly in cold climates and poorly insulated buildings. The heat pump remains the most stable option across most scenarios, despite electricity price variations. With low gas and electricity prices, conventional gas heating results in the lowest fuel costs in most cases, while the IR heating strategy shows the highest costs. Similarly, with high gas and electricity prices, the IR strategy again leads to the highest fuel costs.

However, the most favorable condition for the IR system occurs when electricity prices are low and gas prices are high, which results in the greatest fuel cost savings for the proposed system. This specific price combination is difficult to identify directly from the graph. Therefore, to provide a clear illustration, Figure 4.20 presents the best and worst case fuel cost outcomes for the proposed IR heating strategy. The best case assumes high natural gas prices and low electricity prices, which is seen as a likely future trend due to increasing renewable electricity generation and policies aimed at reducing fossil fuel dependence. In contrast, the worst case assumes low gas prices and high electricity prices.

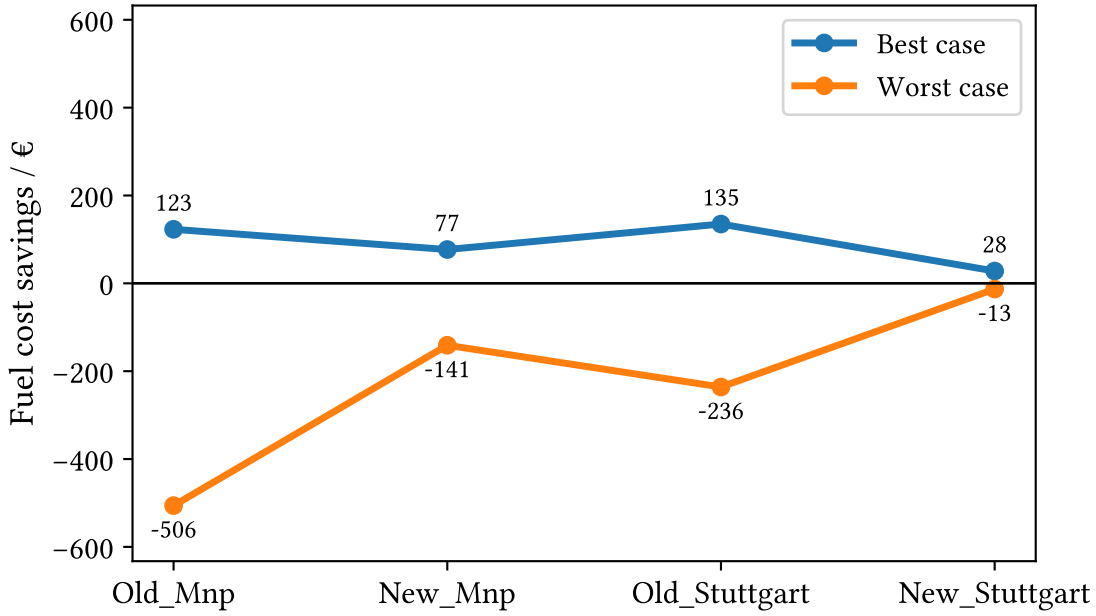

Figure 4.20: Fuel cost savings of the IR heating strategy for the hotel guestroom model with a living room occupancy pattern. The best case represents high gas prices and low electricity prices, while the worst case represents low gas prices and high electricity prices.

As shown, under the best case scenario, the IR heating strategy achieves fuel cost savings across all four scenarios for the hotel model with the living room occupancy pattern. If savings are observed for the longer occupancy pattern, they are expected to be even more apparent for shorter occupancy, such as the dining room pattern. On the other hand, under the worst case scenario, the IR strategy results in higher fuel costs than conventional gas heating in all cases.

In contrast to the living room results, the dining room occupancy pattern gives positive outcomes. The proposed IR heating approach yields the lowest operational fuel cost among the three heating systems across all four scenarios, as shown in Figure 4.21.

Because of the dining room occupancy profile, the IR heater operates less frequently than in the living room, resulting in lower electricity consumption. This reduced operation results in lower fuel costs. Overall, across both models for the short occupancy pattern, the proposed IR strategy leads to lower operational fuel costs, with relative savings ranging from 6% to 40% compared to the reference gas heating.

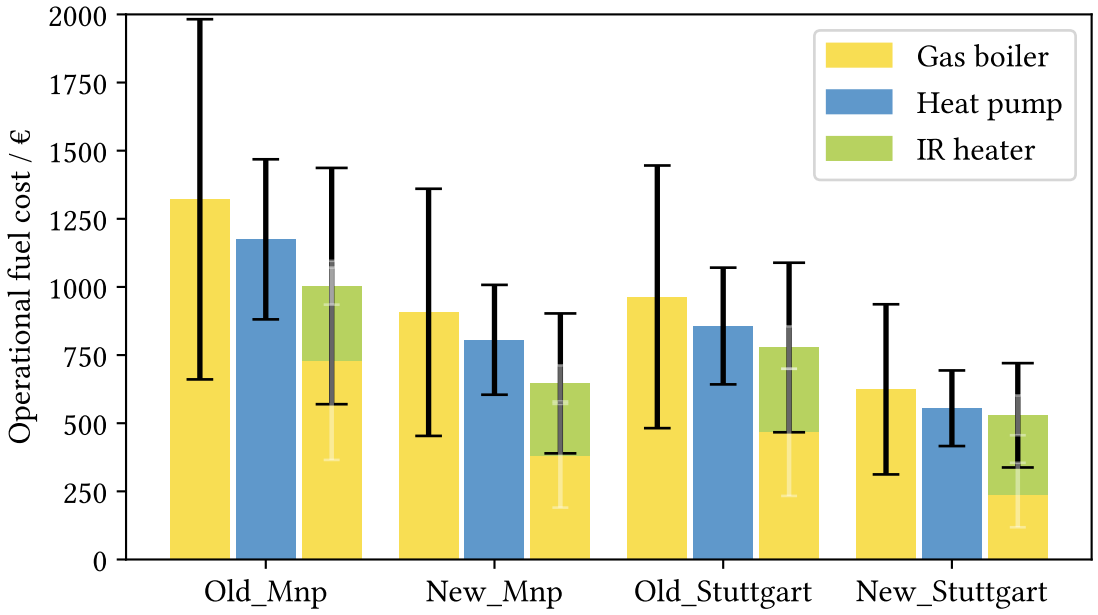

Figure 4.21: Operational fuel cost for the simple house model based on dining room occupancy pattern

The sensitivity analysis further confirms that, with both high and low energy price scenarios, the IR strategy results in the lowest operational fuel costs among all three heating systems. This shows that the proposed approach is the most cost-effective solution for short occupancy patterns. The reduced operating time of the IR heater enables the IR strategy to outperform both conventional gas heating and heat pump systems in terms of fuel costs.

Similar graphical representations for the other two cases (the house model with living room occupancy and the hotel guestroom model with dining room occupancy) are provided in Appendix A-3. The exact numerical values for all cases can be found in Appendix A-2.

4.6 Summary of comparative results

This section summarizes the overall outcomes from the comparison between the proposed IR heating strategy and conventional heating systems across weather types, envelope qualities, and occupancy patterns for both building models.

Impact of building type and heating demand

In general, buildings with higher heating demand, whether due to size, geometry, or being more exposed to the outdoor environment, show greater savings when switching to the new IR heating system. This is evident in the simple house model, where the detached envelope and higher transmission losses result in significantly higher heating requirements. As a result, it gives higher absolute savings. The maximum annual energy reduction for this house reaches 3258 kWh, corresponding to a 37% decrease relative to the reference case. Likewise, this model shows 31% lower annual GHG emissions and around 24% savings in operational fuel costs.

On the other hand, the hotel guestroom model, which is surrounded by adjacent heated rooms,

experiences relatively lower heating demands. consequently, the achievable absolute savings are comparatively smaller. The highest reduction reaches 757 kWh, which corresponds to a 56% decrease relative to the reference base case. Despite the lower absolute reduction, this still represents a significant relative improvement. In addition, 37% lower GHG emissions and about 12% savings in operational fuel costs were observed for the highest energy reduction case of the guestroom model.

Across both models, the new envelope shows the highest efficiency, with energy end use reductions of up to 47% using the IR strategy. However, the absolute impact is smaller because the initial heating demand is already low due to better insulation. This indicates that the proposed strategy is particularly efficient for low-demand buildings. Overall, the results show that higher heating demand leads to greater absolute energy savings when applying the suggested IR heating approach.

Influence of occupancy patterns

For all the cases, scenarios with the dining room occupancy pattern, which represents shorter presence, lead to noticeably higher energy savings. Since the IR heater activates only when occupants are present, this short-duration profile results in substantially fewer operating hours. As a result, unnecessary heating is avoided compared to systems that maintain a full comfort setpoint continuously. This operational behavior leads to comparatively higher savings than in scenarios with a living room or longer occupancy periods. Long duration occupancy results in higher operations of the IR heater, which reduces the relative savings potential.

All of the maximum reductions discussed above for both models were achieved under the dining room occupancy profile. Living room occupancy also leads to reductions in energy use and emissions, although the magnitude is noticeably lower. However, in the case of operational fuel costs, this longer occupancy results in higher expenses across all scenarios because of the increased IR heater activation hours.

Impact of climate type and envelope quality

Across both models, colder climates with poor envelope quality led to significantly higher heating loads, which increases the potential benefit of using an occupancy based IR heating strategy. In such climates, this new system reduces unnecessary heating more effectively, resulting in larger energy savings. However, the impact on emissions and operational costs depends on the respective contribution of base gas heating and IR heater operation within this new approach, meaning that benefits vary depending on how often the IR heater must run.

In milder climates, the relative impact is smaller due to the lower initial heating demand. However, in mild climates with better envelopes, such as the case with the combination of a new envelope and Stuttgart weather, it is observed that under the new heating strategy, the IR heater in combination with the reflective walls can satisfy the entire heating demand. In such situations, there is no need for any base air heating from conventional systems, leading to savings in all forms: energy, operational costs, and emissions.

Overall, the proposed IR heating strategy, which combines IR heaters with reflective interior walls, shows strong energy saving potential compared to conventional gas heating. However, the heat pump offers the most stable performance in terms of GHG emissions and operational fuel costs among the three heating systems.

5. Conclusion and Outlook

The simulation study conducted in this thesis shows that the proposed infrared heating strategy can provide considerable advantages over conventional heating systems. The approach combines a reduced air temperature setpoint, occupancy-controlled and power-modulated IR heating, and reflective wall surfaces. The results include reductions in energy end use, greenhouse gas emissions, and operational fuel costs. These benefits are strongly influenced by building characteristics, occupancy patterns, and climate conditions.

A key finding of this study is that the greatest absolute improvements are achieved in buildings that combine poor envelope performance, short-time occupancy, and strong winter conditions with higher heating demand. Under these conditions, the simple house model, with its fully exposed envelope, demonstrated the largest absolute energy reductions. In this case, the maximum annual saving was 3258 kWh, which corresponds to a 37% decrease compared with the reference gas heating system. Under similar conditions, the hotel guestroom model achieved smaller absolute reductions with a maximum saving of 757 kWh, because it has much lower heating demand due to its surrounding conditioned zones. However, the relative reduction of 56% shows that the proposed heating approach is highly effective in buildings with low overall heating needs.

The occupancy pattern appeared as a decisive factor influencing the performance of the proposed IR heating system. The dining room occupancy profile, presenting a short-duration schedule, consistently delivered greater savings in both building models. Because the IR heater operates in response to occupant presence, a short occupancy profile minimizes unnecessary heating hours and significantly improves energy performance. For the dining room pattern, both models achieved their maximum energy savings. Moreover, the largest absolute GHG emissions reduction of about 31% for the simple house and 37% for the hotel guestroom was also observed with the short-duration occupancy pattern.

Importantly, only the dining room occupancy cases produced positive outcomes regarding operational fuel costs, with the highest absolute cost savings of 24%. In contrast, the living room pattern, presenting long-duration occupancy, reduces the relative advantage of the new heating system, as the IR heater must operate longer to maintain comfort.

Across nearly all scenarios, the proposed system performs better than conventional gas heating in terms of greenhouse gas emissions. In general, a heat pump provides stable results across all scenarios among the three heating systems. Moreover, in scenarios with low-demand and short-duration occupancy profiles, the emissions from the proposed system are even lower than those of a heat pump, demonstrating its potential as the most ecological alternative for such conditions.

Another essential insight is that, with a highly insulated envelope, a moderate climate, and low heating needs, the IR heater and reflective surfaces were sufficient to meet the entire heating demand with only a minor contribution from the base gas heating. Moreover, this configuration resulted in savings across all evaluated parameters, including energy end use, GHG emissions, and operational fuel costs. This indicates that in such low-demand zones, the IR system has the potential to function as a standalone heating solution.

Overall, the findings from this study indicate that the proposed IR heating approach can de-

liver substantial improvements in energy end use, GHG emissions, and operational fuel costs. Short-duration occupancy pattern consistently leads to savings compared to conventional gas heating. Buildings with older envelopes and higher heating demand show larger absolute reductions, resulting in a greater climate impact. In contrast, well-insulated buildings achieve higher relative efficiency, indicating that the proposed IR strategy performs most effectively in low-demand conditions.

The results of this study highlight the potential of infrared heating with reflective walls as an energy-efficient alternative to conventional systems. However, several aspects require further investigation to refine the modeling approach and support real world applications.

In real buildings, reflective wall surfaces would typically be implemented through specialized paints or coatings. The practical performance of such reflective finishes should be evaluated experimentally, considering their interaction with interior furnishings and aesthetic feasibility, to better understand how they influence the performance of the proposed heating approach. A detailed cost assessment is also necessary, including investment costs, maintenance requirements as part of a full life-cycle cost analysis.

The modeling approach should be extended to larger and complex building configurations. Applying this method to multi-zone buildings would provide insights into scalability and control interactions between zones. Additionally, a more detailed representation of the infrared heater is required, considering view factors and radiant distribution patterns.

For a thorough comparison with heat pumps, future work should implement a detailed dynamic heat pump model. This should include part-load performance, defrost cycles, and other operational characteristics that influence the overall energy use and emissions.

6. References

[1] International Energy Agency. *Buildings*. (visited on 14/09/2025). 2025. https://www.iea.org/energy-system/buildings.

[2] Buildings Performance Institute Europe (BPIE). *A Guidebook to European Buildings Efficiency: Key Regulatory and Policy Developments*. Buildings Performance Institute Europe (BPIE), 2022. https://imt.org/wp-content/uploads/2022/02/SPIPA_EU_rev6_508.pdf.

[3] European Commission. *Energy Performance of Buildings Directive*. (visited on 14/09/2025). 2024. https://energy.ec.europa.eu/topics/energy-efficiency/energy-performance-buildings/energy-performance-buildings-directive_en.

[4] European Commission. *European Climate Law*. (visited on 14/09/2025). 2021. https://climate.ec.europa.eu/eu-action/european-climate-law_en.

[5] energieeffiziente Gebäudehülle e.V. (BuVEG). *Wettbewerb „Energieeffizienteste Städte 2023" – Ostdeutschland ist Spitzenreiter*. (visited on 04/12/2025). 2024. https://buveg.de/pressemeldungen/wettbewerb-energieeffizienteste-staedte-2023-ostdeutschland-ist-spitzenreiter/.

[6] European Union. *Directive (EU) 2024/1275 of the European Parliament and of the Council*. (visited on 04/12/2025). 2024. http://data.europa.eu/eli/dir/2024/1275/oj.

[7] Eurostat. *Disaggregated final energy consumption in households – quantities*. (visited on 05/08/2025). https://ec.europa.eu/eurostat/databrowser/product/page/NRG_D_HHQ.

[8] I. E. Agency. *Germany 2025*. Licence: CC BY 4.0. Paris, 2025. https://www.iea.org/reports/germany-2025.

[9] P. P. Altermatt, J. Clausen, H. Brendel, et al. "Replacing gas boilers with heat pumps is the fastest way to cut German gas consumption." In: *Communications Earth & Environment* 4.56 (2023). DOI: https://doi.org/10.1038/s43247-023-00715-7.

[10] A. S. Gaur, D. Z. Fitiwi, and J. Curtis. "Heat pumps and our low-carbon future: A comprehensive review." In: *Energy Research and Social Science* 71 (2021), p. 101764. ISSN: 2214-6296. DOI: https://doi.org/10.1016/j.erss.2020.101764.

[11] International Energy Agency. "The Future of Heat Pumps." In: *International Energy Agency Report* Executive Summary (2022). (visited on 13/09/2025). https://www.iea.org/reports/the-future-of-heat-pumps/executive-summary.

[12] L. Pekař, M. Song, N. Mao, H. M. Ali, W. Wu, and J. Cai. "Editorial: Emerging Sustainable and Energy-Efficient Technologies in Heat Pumps for Residential Heating." In: *Frontiers in Energy Research* 10 (2022). Editorial. DOI: 10.3389/fenrg.2022.866466.

[13] J. H. Lienhard V and J. H. Lienhard IV. *A Heat Transfer Textbook*. 6th. Version 6.00. Cambridge, MA: Phlogiston Press, Apr. 2024. 810 pp. https://ahtt.mit.edu.

[14] U.S. Department of Energy. *Radiant Heating*. (visited on 05/10/2025). Office of Energy Efficiency & Renewable Energy. https://www.energy.gov/energysaver/radiant-heating.

[15] Fraunhofer Institute for Building Physics (IBP). *Vergleichsmessung zwischen elektrischer Infrarotheizung und Gas-Brennwertheizung in zwei baugleichen Einfamilienhäusern*. Aug. 2024. https://ig-infrarot.de/wp-content/uploads/Bericht_IBP_IG-Infrarot_20240812.pdf.

[16] B. W. Olesen. "Radiant floor heating in theory and practice." In: *ASHRAE Journal* 44.7 (2002), pp. 19–24.

[17] J. Heider, N. Conrad, T. Stark, A. Abdulganiev, P. Kosack, and A.-K. Wagner. *Potenzial von Infrarot-Heizsystemen für hocheffiziente Wohngebäude*. Abschlussbericht. Fraunhofer IRB Verlag / Forschungsprojekt IR-Bau (HTWG Konstanz) / BBSR, Zukunft Bau, 2019. https://www.zukunftbau.de/projekte/forschungsfoerderung/1008187-1711.

[18] A. H. H. Ali and M. Gaber Morsy. "Energy efficiency and indoor thermal perception: a comparative study between radiant panel and portable convective heaters." In: *Energy Efficiency* 3 (2010), pp. 283–301. DOI: https://doi.org/10.1007/s12053-010-9077-3.

[19] A. J. H. Corsten. "A Comparative Performance Assessment of Infrared Heating Panels and Conventional Heating Solutions in Dutch Residential Buildings." Master's thesis. Eindhoven, The Netherlands: Eindhoven University of Technology, Aug. 2021. https://research.tue.nl/en/studentTheses/a-comparative-performance-assessment-of-infrared-heating-panels-a/.

[20] P. Kosack. *Beispielhafte Vergleichsmessung zwischen Infrarotstrahlungsheizung und Gasheizung im Altbaubereich*. 2009. https://api.koenighaus-infrarot.de/wp-content/uploads/2018/12/forschungsbericht_ir.pdf.

[21] F. Biliotti. "Performance assessment of heating solution for Dutch residential houses: evaluation of IR-Panels systems and comparison with heat pumps." In: 2020. https://api.semanticscholar.org/CorpusID:237166586.

[22] J. Xu and A. P. Raman. "Controlling radiative heat flows in interior spaces to improve heating and cooling efficiency." In: *iScience* 24.8 (2021), p. 102825. ISSN: 2589-0042. DOI: https://doi.org/10.1016/j.isci.2021.102825.

[23] A. Joudi, A. Sayigh, K. Sopian, M. Alghoul, and M. Wazwaz. "Highly reflective coatings for interior and exterior steel surfaces: Energy minimization study." In: *Applied Energy* 88 (12 2011), pp. 4836–4842. DOI: https://doi.org/10.1016/j.apenergy.2011.06.002.

[24] S. Malz, W. Krenkel, and O. Steffens. "Infrared reflective wall paint in buildings: Energy saving potentials and thermal comfort." In: *Energy and Buildings* 224 (2020), p. 110212. ISSN: 0378-7788. DOI: https://doi.org/10.1016/j.enbuild.2020.110212.

[25] L. A. Wille, B. Schiricke, K. Gehrke, and B. Hoffschmidt. "Reduction of Heating Energy Demand by Combining Infrared Heaters and Infrared Reflective Walls." In: *Buildings* 14.7 (2024), p. 2183. DOI: https://doi.org/10.3390/buildings14072183.

[26] L. A. Wille, B. Schiricke, K. Gehrke, T. Dehne, and B. Hoffschmidt. "Reduction of Heating Energy Demand by Combining IR Heaters and IR Reflective Walls: An Experimental Study." Manuscript under review. 2025.

[27] M. F. Modest. "Chapter 1 - Fundamentals of Thermal Radiation." In: *Radiative Heat Transfer (Third Edition)*. Ed. by M. F. Modest. Third Edition. Boston: Academic Press, 2013, pp. 1–30. ISBN: 978-0-12-386944-9. DOI: https://doi.org/10.1016/B978-0-12-386944-9.50001-7.

[28] *Code of Practice on Energy Efficiency and Use of Renewable Energy for Residential Buildings (2017)*. Tech. rep. Putrajaya, Malaysia: Department of Standards Malaysia, 2017. https://policy.asiapacificenergy.org/node/1268.

[29] J. R. Howell, M. P. Menguc, and R. Siegel. *Thermal Radiation Heat Transfer*. 6th. CRC Press, 2015. DOI: 10.1201/b18835.

[30] A. F. Altun. "Determination of Optimum Building Envelope Parameters of a Room concerning Window-to-Wall Ratio, Orientation, Insulation Thickness and Window Type." In: *Buildings* 12.3 (2022). DOI: https://doi.org/10.3390/buildings12030383.

[31] EnergyPlus Development Team / U.S. DOE. *Zone Internal Gains — EnergyPlus Engineering Reference*. 2024. https://bigladdersoftware.com/epx/docs/9-2/engineering-reference/zone-internal-gains.html.

[32] S. M. Hooshmand, H. Zhang, H. Javidanfar, Y. Zhai, and A. Wagner. "A review of local radiant heating systems and their effects on thermal comfort and sensation." In: *Energy and Buildings* 296 (2023), p. 113331. ISSN: 0378-7788. DOI: https://doi.org/10.1016/j.enbuild.2023.113331.

[33] *International Electrotechnical Vocabulary (IEV) – Part 845: Lighting*. Available at: https://webstore.iec.ch/en/publication/268. Geneva, Switzerland: International Electrotechnical Commission (IEC), 1987.

[34] ICNIRP. *Infrared Radiation — Wavelength Classification and Safety Guidelines*. 2020. https://www.icnirp.org/en/frequencies/infrared/index.html.

[35] S. C. for Research in Built Environment. *Infrared heating: investigations from literature and user trials*. Tech. rep. UK Government Department for Business, Energy & Industrial

Strategy, 2025. https://assets.publishing.service.gov.uk/media/689cd7a7d2a1b0d5d1bb12b1/ir-heating-report.pdf.

[36] *ISO 7730: Ergonomics of the Thermal Environment – Analytical Determination and Interpretation of Thermal Comfort Using Calculation of the PMV and PPD Indices and Local Thermal Comfort Criteria*. Geneva, Switzerland: International Organization for Standardization, 2005. https://www.iso.org/standard/85803.html.

[37] *ANSI/ASHRAE Standard 55: Thermal Environmental Conditions for Human Occupancy*. Atlanta, USA: American Society of Heating, Refrigerating and Air-Conditioning Engineers, 2020. https://www.ashrae.org/technical-resources/bookstore/standard-55-thermal-environmental-conditions-for-human-occupancy.

[38] P. O. Fanger. *Thermal Comfort: Analysis and Applications in Environmental Engineering*. New York, NY, USA: McGraw-Hill, 1970.

[39] G. Fan, Y. Chen, and Q. Deng. "Thermal Comfort." In: *Personal Comfort Systems for Improving Indoor Thermal Comfort and Air Quality*. Indoor Environment and Sustainable Building. Singapore: Springer, 2023, pp. 1–23. DOI: 10.1007/978-981-99-0718-2_1.

[40] P. Fanger, B. Ipsen, G. Langkilde, B. Olessen, N. Christensen, and S. Tanabe. "Comfort limits for asymmetric thermal radiation." In: *Energy and Buildings* 8.3 (1985), pp. 225–236. ISSN: 0378-7788. DOI: https://doi.org/10.1016/0378-7788(85)90006-4.

[41] U.S. Department of Energy. *EnergyPlus — Energy Simulation Software*. Version 24.2.0. 2025. https://energyplus.net/.

[42] U.S. Department of Energy and N. R. E. Laboratory. *EnergyPlus EMS Application Guide*. 2023. https://energyplus.readthedocs.io/en/stable/ems-application-guide/ems-application-guide.html.

[43] I. W. und Umwelt GmbH. *TABULA Web Tool for Building Typology*. 2012. https://www.iwu.de/forschung/gebaeudebestand/tabula/.

[44] EnSimS. *EnSimS — Building Energy Simulation Solutions*. (visited on 05/10/2025). https://app.ensims.com/index.html#!/.

[45] International Code Council. *International Energy Conservation Code (IECC) 2021*. 2021. https://www.iccsafe.org/.

[46] N. R. E. Laboratory. *End-Use Load Profiles for the U.S. Building Stock*. Tech. rep. NREL, 2022. https://www.nrel.gov/buildings/end-use-load-profiles.html.

[47] ASHRAE. *ASHRAE Handbook—Fundamentals*. Atlanta, GA: American Society of Heating, Refrigerating and Air-Conditioning Engineers, 2017. https://www.ashrae.org/technical-resources/ashrae-handbook.

[48] Air Conditioning Contractors of America Association. *Infiltration Guidance for Buildings at Design Conditions*. Tech. rep. ACCA, 2022. https://www.acca.org.

[49] U.S. Department of Energy. *Commercial Reference Buildings*. https://www.energy.gov/eere/buildings/commercial-reference-buildings.

[50] *ANSI/ASHRAE/IES Standard 90.1-2019: High-Performance Energy Design of Low-Rise Residential Buildings*. Atlanta, GA, USA, 2019. https://www.ashrae.org/news/esociety/ansi-ashrae-standard-90-2-high-performance-energy-design-of-residential-buildings.

[51] J. D. Kneifel. *Prototype Residential Buildings for Energy and Sustainability Assessment*. Technical Note TN 1688. Gaithersburg, MD, USA: National Institute of Standards and Technology (NIST), 2011. DOI: https://doi.org/10.6028/NIST.TN.1688.

[52] R. Hendron. *Building America Research Benchmark Definition: Updated December 20, 2007*. Tech. rep. National Renewable Energy Laboratory (NREL), Golden, CO., Dec. 2007. DOI: https://doi.org/10.2172/922141.

[53] Department for Energy Security and Net Zero and Department for Business, Energy & Industrial Strategy. *Cost Optimal Domestic Electrification (CODE): Research Study*. Tech. rep. BEIS Research Paper 2021/051. UK Government, Sept. 2021. https://assets.publishing.service.gov.uk/media/632038fee90e077dba7762a6/CODE-Final-Report-WHOLE-FINAL-v20.pdf.

[54] Eggleston, H.S. and Buendia, L. and Miwa, K. and Ngara, T. and Tanabe, K., ed. *2006 IPCC Guidelines for National Greenhouse Gas Inventories*. Intergovernmental Panel on Climate Change (IPCC), 2006. https://www.ipcc.ch/report/2006-ipcc-guidelines-for-national-greenhouse-gas-inventories/.

[55] U.S. Environmental Protection Agency. *Emission Factors*. (visited on 29/11/2025). https://www.epa.gov/climateleadership/ghg-emission-factors-hub.

[56] H. Johra. *Overview of the Coefficient of Performance (COP) for conventional vapour- compression heat pumps in buildings*. Tech. rep. Jan. 2022. DOI: 10.54337/aau459284067.

[57] Bundesnetzagentur | SMARD.de. *Monitoring Survey 2025*. (visited on 05/12/2025). https://www.smard.de/page/en/topic-article/5892/217372/monitoring-survey-2025.

Appendix

A-1 Available radiant heaters in EnergyPlus

Table 1 provides an overview of the available radiant heating models in EnergyPlus and their compatibility with the Energy Management System (EMS). The table shows that none of the available radiant heater models can be controlled using EMS. These models were initially considered to represent the IR heater in this study. However, because EMS control was crucial for regulating the IR heater power, these models could not be used. As a result, the radiant heater was instead modeled as a simple electric equipment or a plug load, which allows control through EMS and enables the implementation of the proposed control strategy.

Available models for radiant heaters	**EMS compatibility**
ZoneHVAC:Baseboard:RadiantConvective:Electric	✗
ZoneHVAC:LowTemperatureRadiant:Electric	✗
ZoneHVAC:HighTemperatureRadiant	✗

Table 1: EMS compatibility of available radiant models in EnergyPlus

A-2 Additional numerical results

This section contains tables with the exact numerical values of energy use, GHG emissions, and fuel costs for all scenarios discussed, including different heating systems, building models, and occupancy patterns. These values are used to generate all the graphical analyses presented in the main text.

Simple house model with living room occupancy

Scenario	Heating system	Base end use kWh	Gas heating kWh	IR heating kWh
Old_Mnp	Gas heating	700	8648	0
	New IR heating	700	4102	1654
New_Mnp	Gas heating	700	5891	0
	New IR heating	700	1992	1499
Old_Stuttgart	Gas heating	700	6237	0
	New IR heating	700	2316	1835
New_Stuttgart	Gas heating	700	3986	0
	New IR heating	700	1094	1505

Table 2: Energy end use for gas and infrared heating scenarios for the house model with the living room occupancy pattern

Scenario	Heating system	GHG emissions $kg\,CO_2e$	Fuel cost (gas) €	Fuel cost (electricity) €
Old_Mnp	Gas heating	2183	1297	0
	New IR heating	1750	615	662
New_Mnp	Gas heating	1487	884	0
	New IR heating	1150	299	600
Old_Stuttgart	Gas heating	1575	936	0
	New IR heating	1377	347	734
New_Stuttgart	Gas heating	1006	598	0
	New IR heating	926	164	602

Table 3: GHG emissions and fuel costs associated with space heating for the house model with living room occupancy pattern

Simple house model with dining room occupancy

Scenario	Heating system	Base end use kWh	Gas heating kWh	IR heating kWh
Old_Mnp	Gas heating	700	8810	0
	New IR heating	700	4871	682
New_Mnp	Gas heating	700	6045	0
	New IR heating	700	2537	664
Old_Stuttgart	Gas heating	700	6425	0
	New IR heating	700	3109	779
New_Stuttgart	Gas heating	700	4162	0
	New IR heating	700	1577	731

Table 4: Energy end use for gas and infrared heating scenarios for the house model with dining room occupancy pattern

Scenario	Heating system	GHG emissions kg CO_2e	Fuel cost (gas) €	Fuel cost (electricity) €
Old_Mnp	Gas heating	2224	1322	0
	New IR heating	1524	731	273
New_Mnp	Gas heating	1526	907	0
	New IR heating	927	381	265
Old_Stuttgart	Gas heating	1622	964	0
	New IR heating	1121	466	311
New_Stuttgart	Gas heating	1051	624	0
	New IR heating	714	237	293

Table 5: GHG emissions and fuel costs associated with space heating for the house model with dining room occupancy pattern

Hotel guestroom model with living room occupancy

Scenario	Heating system	Base end use kWh	Gas heating kWh	IR heating kWh
Old_Mnp	Gas heating	1068	1970	0
	New IR heating	1068	549	986
New_Mnp	Gas heating	1068	686	0
	New IR heating	1068	83	295
Old_Stuttgart	Gas heating	1068	1156	0
	New IR heating	1068	115	498
New_Stuttgart	Gas heating	1068	160	0
	New IR heating	1068	0	38

Table 6: Energy end use for gas and infrared heating scenarios for the hotel guestroom model with living room occupancy pattern

Scenario	Heating system	GHG emissions kg CO_2e	Fuel cost (gas) €	Fuel cost (electricity) €
Old_Mnp	Gas heating	498	296	0
	New IR heating	564	82	394
New_Mnp	Gas heating	173	103	0
	New IR heating	148	12	118
Old_Stuttgart	Gas heating	292	173	0
	New IR heating	244	17	199
New_Stuttgart	Gas heating	40	24	0
	New IR heating	16	0	15

Table 7: GHG emissions and fuel costs associated with space heating for the hotel guestroom model with living room occupancy pattern

Hotel guestroom model with dining room occupancy

Scenario	Heating system	Base end use kWh	Gas heating kWh	IR heating kWh
Old_Mnp	Gas heating	1068	2160	0
	New IR heating	1068	919	524
New_Mnp	Gas heating	1068	849	0
	New IR heating	1068	175	233
Old_Stuttgart	Gas heating	1068	1361	0
	New IR heating	1068	251	352
New_Stuttgart	Gas heating	1068	257	0
	New IR heating	1068	2	56

Table 8: Energy end use for gas and infrared heating scenarios for the hotel guestroom model with dining room occupancy pattern

Scenario	Heating system	GHG emissions kg CO_2e	Fuel cost (gas) €	Fuel cost (electricity) €
Old_Mnp	Gas heating	545	324	0
	New IR heating	459	138	210
New_Mnp	Gas heating	214	127	0
	New IR heating	145	26	93
Old_Stuttgart	Gas heating	344	204	0
	New IR heating	216	38	141
New_Stuttgart	Gas heating	65	39	0
	New IR heating	25	0	22

Table 9: GHG emissions and fuel costs associated with space heating for the hotel guestroom model with dining room occupancy pattern

A-3 Supplementary fuel cost scenarios

The following figures show additional fuel cost scenarios. These plots follow the same patterns discussed in the main text and are therefore included here for reference.

Hotel guestroom model with dining room occupancy

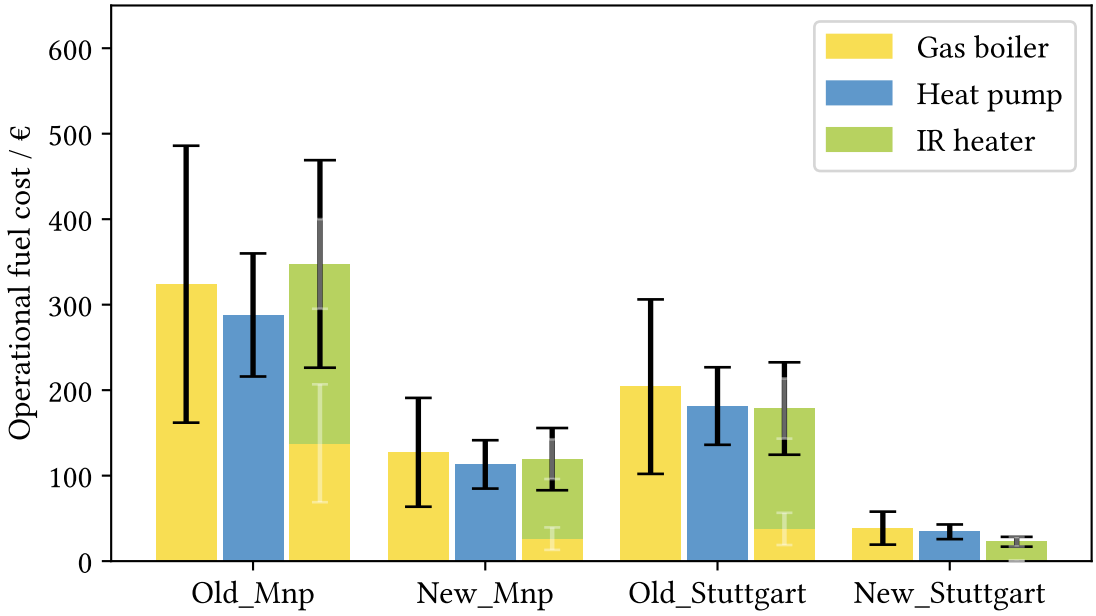

Figure 1: Operational fuel cost for the hotel guestroom model based on dining room occupancy

Simple house model with living room occupancy

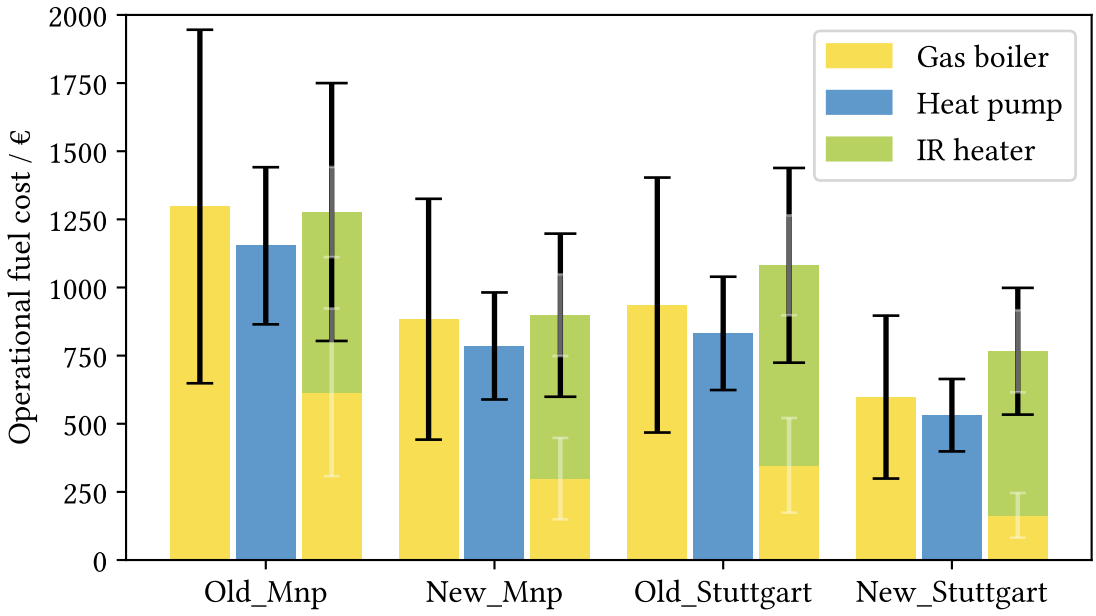

Figure 2: Operational fuel cost for the simple house model based on living room occupancy